

# Osteoarthritis and Cartilage

## Activation of TRPV4 by mechanical, osmotic or pharmaceutical stimulation is anti-inflammatory blocking IL-1 $\beta$ mediated articular cartilage matrix destruction --Manuscript Draft--

<b>Manuscript Number:</b>	OAC10500R2
<b>Article Type:</b>	Manuscript
<b>Keywords:</b>	cartilage; Interleukin-1 $\beta$ ; trpv4; mechanotransduction; mechanobiology; hypo-osmolarity; cilia
<b>Corresponding Author:</b>	Clare Lorraine Thompson, PhD Queen Mary University of London London, UNITED KINGDOM
<b>First Author:</b>	Su Fu, PhD
<b>Order of Authors:</b>	Su Fu, PhD Huan Meng, MD Sheetal Inamdar, PhD Bijoy Das Himadri Gupta, PhD Wen Wang, PhD Clare Lorraine Thompson, PhD Martin M Knight, PhD
<b>Abstract:</b>	<p><b>Objective:</b> Cartilage health is maintained in response to a range of mechanical stimuli including compressive, shear and tensile strains and associated alterations in osmolality. The osmotic-sensitive ion channel Transient Receptor Potential Vanilloid 4 (TRPV4) is required for mechanotransduction. Mechanical stimuli inhibit interleukin-1<math>\beta</math> (IL-1<math>\beta</math>) mediated inflammatory signalling, however the mechanism is unclear. This study aims to clarify the role of TRPV4 in this response.</p> <p><b>Design:</b> TRPV4 activity was modulated (GSK205 antagonist or GSK1016790A (GSK101) agonist) in articular chondrocytes and cartilage explants in the presence or absence of IL-1<math>\beta</math>, mechanical (10% cyclic tensile strain (CTS), 0.33Hz, 24hrs) or osmotic loading (200mOsm, 24hrs). Nitric oxide (NO), prostaglandin E<sub>2</sub> (PGE<sub>2</sub>) and sulphated glycosaminoglycan (sGAG) release and cartilage biomechanics were analysed. Alterations in post-translational tubulin modifications and primary cilia length regulation were examined.</p> <p><b>Results :</b> In isolated chondrocytes, mechanical loading inhibited IL-1<math>\beta</math> mediated NO and PGE<sub>2</sub> release. This response was inhibited by GSK205. Similarly, osmotic loading was anti-inflammatory in cells and explants, this response was abrogated by TRPV4 inhibition. In explants, GSK101 inhibited IL-1<math>\beta</math> mediated NO release and prevented cartilage degradation and loss of mechanical properties. Upon activation, TRPV4 cilia localisation was increased resulting in HDAC6-dependent modulation of soluble tubulin and altered cilia length regulation.</p> <p><b>Conclusion:</b> Mechanical, osmotic or pharmaceutical activation of TRPV4 regulates HDAC6-dependent modulation of ciliary tubulin and is anti-inflammatory. This study reveals for the first time, the potential of TRPV4 manipulation as a novel therapeutic mechanism to suppress pro-inflammatory signalling and cartilage degradation.</p>



School of Engineering and Materials Science  
Queen Mary, University of London  
Mile End Road  
London  
E1 4NS  
United Kingdom

Tel: +44 (0)20 7882 3603  
Fax: +44 (0)20 7882 3390

Tuesday, 04 August 2020

**Re: Article resubmission OAC10500**

To Joel A Block,

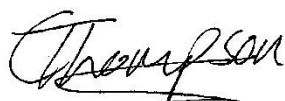
We would like to thank both yourself and the reviewers once again for their careful review of our research article and the constructive feedback they have provided. We have edited the manuscript for clarity and compliance with the word count, included further experimental detail in the methods section and made the corrections identified by reviewer 2.

As discussed via email, we have been unable to incorporate the suggested experimental validation of the TRPV4 antagonist/agonist used in this study within the required timeframe due to the current COVID situation and issues with lab access for our research staff. While we accept these data would add further rigor to our study, it is not expected to change our overall conclusions. The discussion section of the manuscript has been amended to acknowledge this and highlight numerous published studies validating the efficacy of these compounds in chondrocytes.

We hope that with these additional changes you will support publication of this article in *Osteoarthritis & Cartilage*.

We look forward to your response,

Yours sincerely,

A handwritten signature in black ink that reads 'Clare Thompson'.

Clare Thompson

**Reviewer #2:**

1. Although the authors describe that to clarify TRPV4 activation and inactivation by GSK101 and GSK205 is not necessary because these methods using the agonist and antagonist are well established in multiple cell types including chondrocytes, all figures in this paper are based on the activation and inactivation of TRPV4 by using GSK101 and GSK205, respectively. Therefore, the authors must show TRPV4 activation and inactivation by GSK101 and GSK205 as positive and negative control, respectively, using your isolated chondrocytes and cartilage implant.

**Response:**

Reviewer 2 has asked that we conduct a  $Ca^{2+}$  signalling analysis of isolated chondrocytes and cartilage explants in the presence of the TRPV4 agonist GSK1016790A (GSK101) and the antagonist (GSK205) in order to confirm the efficacy of these compounds in modulating channel activity in our hands.

Although our study does not demonstrate the efficacy of these compounds we do provide evidence that they are able to modulate the process of mechanotransduction which is itself dependent on TRPV4  $Ca^{2+}$  channel activity (O'Connor, Leddy et al. 2014). While we accept that confirmation of the efficacy of the TRPV4 agonists/antagonists will add to the rigor of this study however the addition of this data would not change our overall conclusions as significant work demonstrating their specificity/efficacy has been conducted previously (see references below).

The experiments suggested are quite extensive to optimise and then conduct in both isolated cells and cartilage explants. Unfortunately we are unable to perform them in the timeframe offered due to the current covid situation and associated issues with lab access for the researchers on this study. Therefore we have added the additional statement below to the discussion to highlight that GSK205 and GSK101 modulation of  $Ca^{2+}$  signalling has not been analysed in this study but has been shown in numerous previous studies in chondrocytes.

Line 344:

*'...Previous studies demonstrate that GSK101 activates  $Ca^{2+}$  signalling in isolated chondrocytes [17, 48, 56], while GSK205 inhibits this response and blocks  $Ca^{2+}$  signalling in response to mechanical or osmotic loading [18, 57, 58]. While  $Ca^{2+}$  signalling was not assessed in the current study, we hypothesise that elevated  $Ca^{2+}$  levels may regulate HDAC activity...'*

Extensive evidence in the literature confirming the efficacy of GSK205 and GSK101 in chondrocytes as used in the present study:

- Demonstrated that 10  $\mu$ M GSK205 inhibits ligand-gated activation of TRPV4 by ruthenium red or the TRPV4 agonist TRPV4 agonist 4 $\alpha$ PDD in porcine articular chondrocytes (Phan, Leddy et al. 2009).
- Demonstrated activation with 5nM GSK101 by patch clamp electrophysiology could be diminished by 5  $\mu$ M GSK205 inhibitor in porcine articular chondrocytes (Kanju, Chen et al. 2016).
- Demonstrated that in healthy human chondrocytes and chondrocytes isolated from patients with metatropic dysplasia 1  $\mu$ M GSK1016790A activated  $Ca^{2+}$  signalling which could be blocked by 50  $\mu$ M GSK205 (Hurd, Kirwin et al. 2015).
- Demonstrated 100nM GSK101 activated  $Ca^{2+}$  signalling in isolate murine chondrocytes (Servin-Vences, Moroni et al. 2017).
- Demonstrated that 1 nM GSK101 or osmotic loading activated  $Ca^{2+}$  signalling which could be inhibited by 10  $\mu$ M GSK205 in porcine articular chondrocytes (O'Connor, Leddy et al. 2014).

2. There is no explain in Fig. 2D.

**Response:**

The figure legend for Fig.2D reads:

*'(D) confocal microscopy of explants stained with Calcein-AM (live cells, green) and ethidium homodimer (dead cells, red).'*

We have edited the manuscript for clarity, line 188 now reads:

*'Chondrocyte viability was maintained throughout the experiment as determined by live/dead staining.'*

Furthermore, we have added further details of this analysis to the methods section, line 88:

*'For live imaging, cell viability was assessed by live/dead staining at the end of the experimental period. Explants were incubated for 45 min at 37°C with 5 µM Ethidium homodimer-1 (EthD-1) to label dead cells and 5 µM Calcein AM, a marker for live cells.'*

3. Line 189 Fig. 3D ----- > Fig. 2D Is it OK?

**Response:**

We apologise for this error, we have altered the text to the correct figure reference.

4. Fig. 3B: GSK205 ----- > GSK101 Is it OK?

**Response:**

We apologise for this error, this has been corrected in the new figure.

## Activation of TRPV4 by mechanical, osmotic or pharmaceutical stimulation is anti-inflammatory blocking IL-1 $\beta$ mediated articular cartilage matrix destruction

Su Fu, Huan Meng, Sheetal Inamdar, Bijoy Das, Himadri Gupta, Wen Wang, Clare L Thompson\*, Martin M Knight

Institute of Bioengineering, School of Engineering and Materials Science, Queen Mary University of London

\* Corresponding author:

Dr Clare Thompson,

School of Engineering and Materials Science,

Queen Mary University of London,

Mile End Road, London, E1 4NS, UK

Email: [Clare.l.thompson@qmul.ac.uk](mailto:Clare.l.thompson@qmul.ac.uk)

Tel: 020 7882 3603

### Co-author email addresses:

Su Fu	<a href="mailto:s.fu@qmul.ac.uk">s.fu@qmul.ac.uk</a>
Huan Meng	<a href="mailto:Huan.meng@qmul.ac.uk">Huan.meng@qmul.ac.uk</a>
Sheetal Inamdar	<a href="mailto:s.r.inamdar@qmul.ac.uk">s.r.inamdar@qmul.ac.uk</a>
Himadri Gupta	<a href="mailto:h.gupta@qmul.ac.uk">h.gupta@qmul.ac.uk</a>
Wen Wang	<a href="mailto:Wen.wang@qmul.ac.uk">Wen.wang@qmul.ac.uk</a>
Clare L Thompson	<a href="mailto:Clare.l.thompson@qmul.ac.uk">Clare.l.thompson@qmul.ac.uk</a>
Martin M Knight	<a href="mailto:m.m.knight@qmul.ac.uk">m.m.knight@qmul.ac.uk</a>

### Abstract

**Objective:** Cartilage health is maintained in response to a range of mechanical stimuli including compressive, shear and tensile strains and associated alterations in osmolality. The osmotic-sensitive ion channel Transient Receptor Potential Vanilloid 4 (TRPV4) is required for mechanotransduction. Mechanical stimuli inhibit interleukin-1 $\beta$  (IL-1 $\beta$ ) mediated inflammatory signalling, however the mechanism is unclear. This study aims to clarify the role of TRPV4 in this response.

**Design:** TRPV4 activity was modulated (GSK205 antagonist or GSK1016790A (GSK101) agonist) in articular chondrocytes and cartilage explants in the presence or absence of IL-1 $\beta$ , mechanical (10% cyclic tensile strain (CTS), 0.33Hz, 24hrs) or osmotic loading (200mOsm, 24hrs). Nitric oxide (NO), prostaglandin E<sub>2</sub> (PGE<sub>2</sub>) and sulphated glycosaminoglycan (sGAG) release and cartilage biomechanics were analysed. Alterations in post-translational tubulin modifications and primary cilia length regulation were examined.

**Results:** In isolated chondrocytes, mechanical loading inhibited IL-1 $\beta$  mediated NO and PGE<sub>2</sub> release. This response was inhibited by GSK205. Similarly, osmotic loading was anti-inflammatory in cells and explants, this response was abrogated by TRPV4 inhibition. In explants, GSK101 inhibited IL-1 $\beta$  mediated NO release and prevented cartilage degradation and loss of mechanical properties. Upon

activation, TRPV4 cilia localisation was increased resulting in HDAC6-dependent modulation of soluble tubulin and altered cilia length regulation.

Conclusion: Mechanical, osmotic or pharmaceutical activation of TRPV4 regulates HDAC6-dependent modulation of ciliary tubulin and is anti-inflammatory. This study reveals for the first time, the potential of TRPV4 manipulation as a novel therapeutic mechanism to suppress pro-inflammatory signalling and cartilage degradation.

**Key words**

Cartilage, IL-1 $\beta$ , TRPV4, mechanotransduction, mechanobiology, hypo-osmolarity, cilia

**Running headline**

TRPV4 activation suppresses inflammation

[Click here to view linked References](#)

## 1 **Introduction**

2 Osteoarthritis (OA) affects over 4.4 million people in the UK alone representing significant  
3 economic cost [1]. Cartilage health is maintained in response to mechanical stimuli, articular  
4 cartilage is routinely exposed to a wide array of dynamic mechanical loading consisting of  
5 compressive, shear and tensile strains as well as associated alterations in fluid shear and  
6 osmolality [2]. Mechanical loading in the form of compression or tensile strain is anti-  
7 inflammatory in chondrocytes and blocks the release of the pro-inflammatory mediator's  
8 nitric oxide (NO) and prostaglandin E<sub>2</sub> (PGE<sub>2</sub>) in response to interleukin-1 $\beta$  (IL-1 $\beta$ ) [3-5].  
9 Inflammatory signalling contributes to cartilage degradation in OA thus understanding the  
10 link between mechanical loading and inflammation will have significant therapeutic impact.

11 The osmotic-sensitive Ca<sup>2+</sup> ion channel Transient Receptor Potential Vanilloid 4 (TRPV4) is  
12 highly expressed in articular chondrocytes and is activated by mechanical stimuli [6, 7].  
13 TRPV4 is required for mechanotransduction in chondrocytes and other cells types [7-9]. It  
14 mediates the regulation of pro-anabolic and anti-catabolic genes promoting matrix  
15 production and accumulation in agarose-embedded chondrocytes [7, 9]. TRPV4 mutations  
16 result in human skeletal dysplasia suggesting a role in bone development (for review see  
17 [10]). Indeed, chondrocytes from TRPV4<sup>-/-</sup> mice exhibit loss of osmosensitivity accompanied  
18 by joint degeneration indicating a central role for this channel protein in maintaining joint  
19 homeostasis [11, 12]. Pharmaceutical activation of TRPV4 inhibits NO release in response  
20 to inflammatory cytokines suggesting a potential mechanistic role in the anti-inflammatory  
21 effects of mechanical loading [13, 14]. However, in apparent contradiction of these findings  
22 TRPV4 inhibition exerts an anti-inflammatory effect in the cardiovascular system, lung and  
23 peripheral nervous system [15-17]. This study therefore aims to clarify the regulatory role of  
24 TRPV4 in cartilage inflammatory signalling.

25 TRPV4 localises to the plasma membrane and primary cilium, a small microtubule based  
26 signalling compartment present at the cell surface [18, 19]. Primary cilia have been

27 implicated in both chondrocyte mechanotransduction [20-22] and inflammatory signalling  
28 [23-26]. The cytoplasmic tubulin deacetylase histone deacetylase 6 (HDAC6) is enriched  
29 within the cilium and modulates cilia resorption through de-acetylation and polymerization of  
30 ciliary tubulin [27-29]. Post translational modification of ciliary tubulin influences intraflagellar  
31 transport (IFT), the microtubule based motility present within the cilium required for cilia-  
32 mediated signalling [30, 31]. Previously we report that mechanical loading counteracts  
33 inflammatory signalling in response to the pro-inflammatory cytokine interleukin 1 $\beta$  (IL-1 $\beta$ )  
34 via HDAC6 activation in association with alterations in IFT/cilia [5]. A role for TRPV4 in this  
35 pathway has not previously been identified.

36 In the present study, we demonstrate for the first time that TRPV4 activation by cyclic tensile  
37 strain, hypo-osmotic challenge or the TRPV4 agonist GSK1016790A inhibits pro-  
38 inflammatory IL-1 $\beta$  signalling and cartilage degradation associated with alterations in primary  
39 cilia elongation. TRPV4 may therefore provide a novel target for the treatment of joint  
40 disease and other inflammatory pathologies.

## 41 **Methods**

### 42 **Antibodies and reagents**

43 Chondrocytes were treated with interleukin-1 $\beta$  (IL-1 $\beta$ , 200-01B; Peprotech, London, UK),  
44 TRPV4 antagonist GSK205 (616522; Merck Millipore, London, UK) and agonist  
45 GSK1016790A (GSK101, G0798; Sigma Aldrich, Poole, UK). Antibodies for  
46 immunocytochemistry: acetylated  $\alpha$ -tubulin (1:2000, T7451, Sigma Aldrich, Poole, UK) and  
47 TRPV4 (1:200, SAB2104243, Sigma Aldrich). Nuclei were counterstained with 4',6-  
48 diamidino-2-phenylindole (DAPI, Sigma Aldrich). Antibodies for western blotting: acetylated  
49  $\alpha$ -tubulin (1:1000, T7451, Sigma Aldrich) and  $\alpha$ -tubulin (1:1000, ab4074, Abcam, Cambridge,  
50 UK).

### 51 **Cartilage explant and chondrocyte culture**



52 Bovine cartilage explants and chondrocytes were obtained from 16 month steers as  
53 previously described [28]. Full depth articular cartilage was removed from the proximal  
54 surface of the metacarpal phalangeal joint and chondrocytes isolated by enzymatic  
55 digestion. Explants were harvested using a 5 mm diameter biopsy punch (BP-50F, Selles  
56 Medical Ltd, UK). Both were cultured at 37 °C, 5% CO<sub>2</sub> in Dulbeccos Minimal Essential  
57 Medial (DMEM, D5921, Sigma-Aldrich, Poole, UK) supplemented with 10% (v/v) foetal calf  
58 serum (FCS, F7524, Gibco, Paisley, UK), 1.9 mM L-glutamine (G7513), 96 U/ml penicillin  
59 (P4333, All Sigma-Aldrich, Poole, UK). Explants were rested for 2 d prior to experimentation  
60 while isolated chondrocytes were cultured to confluence.

### 61 **Application of cyclic tensile strain**

62 Isolated chondrocytes were cultured on collagen coated flexible elastomeric membranes and  
63 subjected to uniform, equibiaxial cyclic tensile strain (CTS) applied using the Flexcell 5000T  
64 system (Dunn Labortechnik GmbH). Cells were subjected to 0-10% strain for 24 h at 0.33 Hz.

### 65 **Application of osmotic loading**

66 Isolated cells were cultured for 24 h without serum in osmotically adjusted media at 200, 315  
67 or 400 mOsm, hereafter referred as hypo-, iso- or hyper- osmotic media respectively.  
68 Explants were cultured for up to 12 d under similar conditions with the addition of serum to  
69 maintain chondrocyte viability resulting in a slightly higher osmolarity of 318 mOsm for the  
70 iso-osmotic media. The osmolarity of all solutions was adjusted by adding D-mannitol  
71 (M4125, Sigma-Aldrich) or distilled water and measured using a freezing point depression  
72 osmometer.

### 73 **Biochemical analysis of NO, PGE<sub>2</sub> and sGAG release**

74 Nitric Oxide (NO) release was assessed using the Griess assay based on quantification of  
75 nitrite (NO<sub>2</sub>), the stable product of NO degradation. Nitrite content was quantified against a  
76 sodium nitrite standard curve using the Galaxy Fluorstar spectrophotometer (BMG Labtech,

77 UK). An immunoassay kit (KGE004B, R&D Systems, UK) was used to quantify PGE<sub>2</sub>  
78 concentrations in the media according to the manufacturer's instructions. Results were  
79 corrected for non-specific binding and calibrated using a PGE<sub>2</sub> standard curve. The release  
80 of sGAG into the culture media was quantified using the dimethylmethylenesblue (DMMB)  
81 assay against a chondroitin sulphate standard curve (6-sulphate:4-sulphate; 0.33:1; Sigma–  
82 Aldrich).

### 83 **Immunocytochemistry, live imaging and confocal microscopy**

84 For immunocytochemistry, samples were fixed with 4% paraformaldehyde for 10 min,  
85 permeabilised for 5 min with 0.5% triton-X100/phosphate buffered saline (PBS) then blocked  
86 with 5% goat serum/PBS for 1 h. Primary antibody was incubated at 4°C overnight followed  
87 by appropriate Alexa Fluor conjugated secondary antibodies (Molecular Probes) for 1 h at  
88 room temperature. Cells were counterstained with 1 µg/ml DAPI for 5 min. For live imaging,  
89 cell viability was assessed by live/dead staining. Explants were incubated for 30 min with 5  
90 µM Calcein AM and 5 µM Ethidium homodimer-1 (EthD-1) prepared in appropriate osmotic  
91 adjusted media, washed and immediately imaged. Samples were imaged using a Zeiss 710  
92 ELYRA PS.1 microscope. For cilia analysis, samples were imaged using an x63/1.4 NA  
93 objective to generate confocal z-sections made throughout the cell depth (approximately 20  
94 sections) using 0.25 µm step size with an image format of 1024 x 1024 yielding a pixel size  
95 of 0.13 x 0.13 µm (image size approximately 135 x 135 µm). Cilia length and prevalence was  
96 quantified from resulting maximum projection images using Image J software (National  
97 Institutes of Health, Maryland, USA).

### 98 **Western blotting**

99 Cells were lysed in RIPA buffer (R0278, Sigma Aldrich) and total protein quantified by  
100 Bicinchoninic acid (BCA) assay. For the fractionation of soluble and polymerized tubulin,  
101 extraction buffer A (137 mM NaCl, 20 mM Tris-HCl, 1% Triton X-100, and 10% glycerol) was  
102 added to cells at 4 °C for 3 min, plates were gently swirled and the buffer removed and

103 saved as the soluble tubulin fraction. Immediately after, extraction buffer B (buffer A + 1%  
104 SDS) was added for 1 min, the remaining sample was scraped, incubated on ice for 30 min  
105 and saved as the polymerized tubulin fraction.

106 SDS-PAGE was performed under reducing conditions and proteins transferred to  
107 nitrocellulose membranes. Membranes were blocked in odyssey blocking buffer (Li-Cor  
108 Cambridge, UK) prior to overnight incubation with primary antibodies and infrared secondary  
109 antibodies (Li-Cor). Proteins were visualized using the Li-Cor Odyssey and quantified using  
110 Image Studio Lite software (Li-Cor).

### 111 **HDAC6 activity measurement**

112 A commercial fluorometric assay kit (K466-100, Biovision) was used to measure HDAC6  
113 activity according to the manufacturer's instructions. This assay determines enzyme activity  
114 by exploiting the selectivity of tubacin for HDAC6 in combination with a fluorescent synthetic  
115 acetylated-peptide substrate. Cultures were lysed, a 10 µl aliquot was mixed with either  
116 acetylated substrate (sample) or with 2 µM tubacin and acetylated substrate (inhibitor  
117 control) then incubated for 30 min at 37°C. The deacetylase-dependent release of a 7-  
118 amino-4-trifluoromethylcoumarin fluorophore (excitation/emission at 350/490 nm) was then  
119 measured on a Galaxy Fluorstar spectrophotometer (BMG Labtech, UK) and HDAC6 activity  
120 calculated as [sample-inhibitor control].

### 121 **Mechanical testing of cartilage explants**

122 The mechanical behaviour of individual cartilage explants was measured using an MTS,  
123 Bionix 100. A 2 mm diameter core was cut from the centre of each 5 mm diameter cartilage  
124 explant and a tare load of 0.01 N applied to each explant which was then hydrated in culture  
125 media. The explants were subjected to a 20% uniaxial unconfined compressive strain (20%  
126 /min). This was followed by a stress relaxation period at constant 20% strain in which the  
127 load was recorded for a further 300 s. The load was recorded throughout the test at a

128 sampling frequency of 60 Hz. Stress–strain and stress–time curves were generated for each  
129 specimen and the following mechanical properties of the cartilage determined:

130 Tangent Modulus (MPa) =  $\frac{\sigma_{\varepsilon=0.2} - \sigma_{\varepsilon=0.18}}{0.02}$

131 Relaxation Modulus (MPa) =  $\frac{\sigma_{t=300s}}{0.2}$

132 Percentage Relaxation (%) =  $\frac{\sigma_{t=0s} - \sigma_{t=300s}}{\sigma_{t=0s}}$

133 The relaxation half-life was calculated as the time from the start of the relaxation phase until  
134 stress reduced to half the peak value.

### 135 **Statistical analyses**

136 The sample size for each experiment was chosen based on previous studies [5, 32] where  
137 analysis of cartilage degradation by biochemistry, immunohistochemistry and mechanical  
138 testing demonstrated that 6-8 samples/group is sufficient to detect a 25% difference in  
139 cartilage matrix catabolism at 80% power and a significance of  $p < 0.05$ . Data analysis was  
140 conducted using GraphPad Prism version 8 (GraphPad software, La Jolla California USA,  
141 [www.graphpad.com](http://www.graphpad.com)). Normality testing (Kolmogorov Smirnov test) was performed to confirm  
142 that data exhibited Gaussian distribution. For data sets that were not normally distributed,  
143 namely cilia length data, Box Cox transformation ( $\lambda=0.5$ ) was performed prior to statistical  
144 analyses. Statistical significance was determined by T-Test, One-way, Two-way or Three-  
145 way ANOVA as appropriate with post-hoc Tukey's multiple comparisons performed to  
146 identify significant differences between groups. Statistically significant differences were  
147 determined based on a threshold of \* =  $p < 0.05$ , \*\* =  $p < 0.01$  and \*\*\* =  $p = 0.001$ . Data is  
148 presented as mean  $\pm$  standard deviation (SD) unless otherwise stated.

149 **Results**

150 **TRPV4 activation is required for the anti-inflammatory effects of mechanical loading**  
151 **in isolated chondrocytes**

152 IL-1 $\beta$  treatment (24 h) resulted in significant, dose-dependent release of NO and PGE<sub>2</sub> (Fig.  
153 1AB, S1AB). In response to 1 ng/ml IL-1 $\beta$  isolated chondrocytes exhibited a 3.04-fold  
154 increase in nitrite levels indicative of NO release (Fig. 1A), and a 4.84-fold increase in PGE<sub>2</sub>  
155 release (Fig. 1B) which increased to 11.48- and 7.37-fold respectively in response to 10  
156 ng/ml IL-1 $\beta$  (Fig. S1A-B). Consistent with previous studies [5] this response was significantly  
157 reduced by mechanical loading in the form of CTS. IL-1 $\beta$  induced NO release was abolished  
158 by CTS such that there was no statistically significant effect at either 1 or 10 ng/ml (Fig. 1A,  
159 S1A). PGE<sub>2</sub> release was completely inhibited by CTS at 1 ng/ml IL-1 $\beta$  (Fig. 1B) but only  
160 partially suppressed at 10 ng/ml (Fig. S1B).

161 Simultaneous treatment with the TRPV4 antagonist GSK205 (10  $\mu$ M) abolished the anti-  
162 inflammatory effects of mechanical loading (Figure 1, S1). While GSK205 had no effect on  
163 NO or PGE<sub>2</sub> release in unloaded cells with or without IL-1 $\beta$ , in loaded cells the IL-1 $\beta$   
164 response was restored such that NO (Fig. 1A and S1A) and PGE<sub>2</sub> release (Fig. 1B, S1B)  
165 were significantly increased by IL-1 $\beta$ . Neither IL-1 $\beta$  nor GSK205 treatment in the presence  
166 or absence of CTS influenced TRPV4 protein levels (Fig. S10). These data indicate the anti-  
167 inflammatory effects of mechanical loading are mediated by TRPV4 activation.

168 **TRPV4 activation is required for the anti-inflammatory effects of hypo-osmotic loading**  
169 **in isolated chondrocytes and cartilage explants**

170 Isolated chondrocytes were treated with hyper-osmotic media (400 mOsm), hypo-osmotic  
171 (200 mOsm) or iso-osmotic media (315 mOsm) for 24 h (Figure 2AB, S2). Hyper-osmotic  
172 challenge had no significant effect on NO release, with or without IL-1 $\beta$  relative to the iso-  
173 osmotic control (Fig. S2, S3). By contrast, hypo-osmotic challenge significantly attenuated

174 the pro-inflammatory response to IL-1 $\beta$  (1 ng/ml), such that the increase in NO release at 24  
175 h was significantly reduced ( $p < 0.001$ , Fig. 2A S2A). Hypo-osmotic challenge had no  
176 apparent effect on cell viability compared to control conditions based on brightfield  
177 microscopy (Figure 2B). In the presence of GSK205, the anti-inflammatory effect of hypo-  
178 osmotic challenge on IL-1 $\beta$  induced NO release was completely inhibited by GSK205 such  
179 that the induction of NO release was not significantly different to control conditions (Fig. 2A).  
180 In the absence of IL-1 $\beta$ , GSK205 also had no effect on baseline NO or PGE<sub>2</sub> levels (Fig.  
181 S2).

182 In cartilage explants, hypo-osmotic challenge significantly reduced IL-1 $\beta$  induced NO release  
183 (Fig. 2C,  $p < 0.001$ ) such that there was no significant difference between IL-1 $\beta$  treated and  
184 untreated explants (Fig. 2C, S4A). In line with these findings hypo-osmotic challenge  
185 blocked the IL-1 $\beta$  mediated release of sGAG into the media, indicative of a reduction in  
186 extracellular matrix degradation (Fig. S4B). Chondrocyte viability was maintained throughout  
187 the experiment as determined by live/dead staining (Fig. 2D). Consistent with isolated cells,  
188 hyper-osmotic challenge (400 mOsm, 12 d) had no effect on NO or sGAG release in the  
189 presence or absence of 1 ng/ml IL-1 $\beta$  (Fig. S4). GSK205 treatment restored IL-1 $\beta$ -induced  
190 NO release in hypo-osmotic media (Fig. 2C) thus blocking the anti-inflammatory effect of  
191 osmotic challenge. Interestingly, GSK205 further increased IL-1 $\beta$ -induced NO release in iso-  
192 osmotic, control media a response not seen in isolated cells (Fig. 2C). Together these data  
193 indicate the anti-inflammatory effects of hypo-osmotic loading are also mediated by TRPV4  
194 activation.

## 195 **TRPV4 activation is associated with altered primary cilia localisation and regulates** 196 **cilia length**

197 IL-1 $\beta$  induces primary cilia elongation in articular chondrocytes and mediates downstream  
198 catabolic NF- $\kappa$ B signalling through regulation of IFT [5, 23, 24]. We therefore examined the  
199 involvement of primary cilia in the anti-inflammatory mechanism of TRPV4 activation. TRPV4

200 cilia localisation was observed in isolated chondrocytes (Fig 3A). TRPV4 activation by  
201 mechanical loading, hypo-osmotic challenge or the TRPV4 agonist GSK101 (1 nM)  
202 increased TRPV4 cilia localisation while not significantly affecting protein expression, as  
203 shown by the increased mean intensity of ciliary TRPV4 (Fig. 3B, S10) and altered  
204 distribution profile of TRPV4 in proximal and distal regions of the axoneme (Fig. 3C) these  
205 data are suggestive of alterations in IFT.

206 In isolated chondrocytes, IL-1 $\beta$  (1 ng/ml) treatment for 24 h induced a significant increase in  
207 primary cilia length ( $p < 0.001$ ) from a median value of 2.21 to 2.84  $\mu\text{m}$ . This elongation was  
208 abolished by TRPV4 activation with GSK101 (Fig. 3D-E). IL-1 $\beta$  mediated cilia elongation  
209 was also blocked by mechanical loading (CTS, 0-10%, 0.33 Hz, Fig. 3G) and hypo-osmotic  
210 challenge (Fig 3H). Inhibition of TRPV4 with GSK205 restored IL-1 $\beta$  mediated cilia  
211 elongation in the presence of both mechanical loading ( $p < 0.001$ , Fig. 3G), and hypo-osmotic  
212 challenge ( $p < 0.001$ , Fig. 3H). GSK101, had no effect on cilia length in iso-osmotic conditions  
213 with or without IL-1 $\beta$  (Fig. 3E). GSK101 also had no effect on cilia prevalence for any of the  
214 treatment groups (Fig. S5A and D).

### 215 **TRPV4 activation inhibits inflammatory signalling in response to IL-1 $\beta$ through the** 216 **regulation of HDAC6 and ciliary tubulin**

217 We next examined whether direct pharmaceutical activation of TRPV4 would replicate the  
218 anti-inflammatory effect of mechanical and osmotic loading. IL-1 $\beta$  (1 ng/ml) induced the  
219 characteristic upregulation of NO and PGE<sub>2</sub> release in isolated chondrocytes which was  
220 abolished by GSK101 (Fig. 4A and B). Similarly IL-1 $\beta$  induced COX2 expression was  
221 abolished by GSK101 (Fig. 4C). No effects on cell viability based on bright field microscopy  
222 (Fig. S6A) and DNA content were observed although cells appeared to have a more rounded  
223 morphology particularly at high concentrations (Fig. S6B).

224 Previously, we identified a mechanistic role for HDAC6 activation and post-transcriptional  
225 tubulin modifications in the anti-inflammatory effect of mechanical loading [5]. Similarly,

226 GSK101 resulted in significant upregulation of HDAC6 activity (Fig. 4D) suggesting TRPV4-  
227 mediated calcium signalling activates HDAC6. Consistent with this finding we observed  
228 significant tubulin deacetylation accompanied by a reduction in the pool of non-polymerized,  
229 soluble tubulin (Fig. 4E-F). Furthermore, the HDAC6 specific inhibitor, tubacin (500 nM),  
230 restored IL-1 $\beta$  mediated stimulation of NO release in GSK101-treated cells (Fig. 4G). These  
231 data suggest that GSK101 mimics the effects of mechanical loading on IL-1 $\beta$  inflammatory  
232 signalling, HDAC6 activation and tubulin modification.

### 233 **TRPV4 activation abolishes IL-1 $\beta$ mediated cartilage degradation and loss of** 234 **mechanical properties**

235 We next determined whether pharmaceutical activation of TRPV4 could prevent cartilage  
236 degradation and loss of mechanical properties. Cartilage explants were treated with IL-1 $\beta$  for  
237 up to 12 d in the presence of 1 nM or 10 nM GSK101. Cartilage explant viability was  
238 maintained at these experimental doses (Fig. S7). In response to IL-1 $\beta$  treatment, significant  
239 NO release was observed (Fig. 5A,  $P < 0.001$ ) indicative of activation of inflammatory  
240 signalling. This response was accompanied by significant sGAG release indicative of  
241 cartilage degradation (Fig. 5B,  $P < 0.001$ ).

242 We measured the viscoelastic properties of cartilage tissue using uniaxial unconfined  
243 compression to determine whether GSK101 could prevent the loss of mechanical properties  
244 induced by IL-1 $\beta$ . Cartilage explants exhibited a non-linear stress-strain graph represented  
245 by a tangent modulus of 15-20MPa (Fig 5C). This was followed by characteristic viscoelastic  
246 stress relaxation at 20% strain (Fig 5D) to a relaxation modulus of 2-3 MPa at 300 s  
247 representing 80% relaxation and a relaxation half-life of approximately 50 s (Fig. 5E-H). IL-  
248 1 $\beta$  treatment resulted in dramatic loss of mechanical stiffness as shown by significant  
249 reductions in tangent modulus ( $p < 0.001$ , Fig. 5E) and relaxation modulus ( $p < 0.001$ , Fig. 5F),  
250 increased percentage relaxation ( $p < 0.001$ , Fig. 5G) and a reduction in half-life ( $p < 0.001$ , Fig.  
251 5H).



252 GSK10 significantly inhibited the cumulative release of NO from cartilage explants in  
253 response to IL-1 $\beta$  treatment ( $p < 0.001$ , Fig. 5A). Similarly the cumulative release of sGAG  
254 was significantly reduced ( $p < 0.001$ ) and loss of mechanical properties in response to IL-1 $\beta$   
255 abolished, such that there was no significant difference in any of the biomechanical  
256 parameters with and without IL-1 $\beta$ .

## 257 **Discussion**

258 This study demonstrates that TRPV4 plays an important mechanistic role in the anti-  
259 inflammatory effect of mechanical stimulation. TRPV4 inhibition restores IL-1 $\beta$  mediated pro-  
260 inflammatory signalling in the presence of both mechanical and osmotic loading. Conversely,  
261 TRPV4 activation by GSK101 blocked the release of pro-inflammatory mediators in the  
262 absence of load in isolated cells and prevented cartilage degradation and loss of mechanical  
263 properties in an explant model. TRPV4 is activated by mechanical stimulation in the form of  
264 cyclic tensile strain or osmotic challenge and functions upstream of HDAC6 to modulate  
265 tubulin acetylation and polymerization which regulates IFT thereby suppressing IFT-  
266 dependent IL-1 $\beta$  signalling.

267 TRPV4 is expressed in bone marrow stem cells, osteoblasts, osteoclasts and chondrocytes,  
268 and is required for skeletal development [10, 33]. TRPV4 belongs to the Transient Receptor  
269 Potential (TRP) superfamily which mediate cellular responses to a variety of environmental  
270 stimuli including heat [34], cell swelling [35], hypo-osmolality [18, 36] and mechanical  
271 loading [7, 9] and results in elevated levels of intracellular Ca<sup>2+</sup>. Thus, TRPV4 is required for  
272 mechanotransduction. It promotes chondrocyte matrix production in response to dynamic  
273 compression [7], mediates the fluid shear induced osteogenic response in stem cells [9] and  
274 shear stress induced vasodilatation in endothelial cells [8].

275 In other tissues, TRPV4 activation is mostly reported to be pro-inflammatory. In airway  
276 epithelial cells, TRPV4 activates NF- $\kappa$ B signalling promoting progression of lung fibrosis [37].  
277 Endogenous TRP channel agonists are detected in a lung injury model while TRPV4

278 inhibition suppresses acid-induced pulmonary inflammation [38]. TRPV4 antagonists have  
279 been used to treat sepsis in mice by reducing production of TNF- $\alpha$ , IL-1 and IL-6 [16].  
280 Moreover loss of TRPV4 function suppresses inflammatory fibrosis in mouse corneas [39].  
281 However, Xu et al. report that GSK101 prevents vascular inflammation and atherosclerosis,  
282 associated with inhibition of NO synthase and MAPK signalling [14]. TRPV4 is also well-  
283 established to mediate inflammatory hyperalgesia (see review [40]) and is regarded as a  
284 promising target for novel analgesics.

285 Consistent with our findings, pharmaceutical activation of TRPV4 has been shown to  
286 suppress NO release induced by lipopolysaccharide (LPS) in rat temporomandibular  
287 chondrocytes, whereas TRPV4 inhibition aggravates the inflammatory response to LPS  
288 [13]. Clark et al. report that TRPV4 deficiency induces inflammation and disrupts cartilage  
289 matrix homeostasis. As such, TRPV4<sup>-/-</sup> mice exhibit a severe sex-dependent osteoarthritis  
290 (male mice are more susceptible) while the isolated chondrocytes fail to increase Ca<sup>2+</sup> influx  
291 in response to hypo-osmotic challenge [11]. These mice exhibit a more severe obesity-  
292 induced osteoarthritis, compared to wild-type mice [12]. However other studies report  
293 osmotic challenge to be a pro-inflammatory signal. Hubert et al observed induction of IL-8 in  
294 response to both hyper and hypo-osmotic stress [41] while hypo-osmotic stimulation of  
295 TRPV4 promoted PGE<sub>2</sub> release in porcine chondrocytes [18] and the expression of IL-1 $\beta$   
296 and IL-6 in bovine intervertebral disc cells [36], suggesting a pro-inflammatory role of  
297 TRPV4. We did observe a mild, transient increase in NO release in this study at 3 h hypo-  
298 osmotic challenge however this had resolved and was not significantly different to the control  
299 at 24 h (Fig. S8). Interestingly we observed dose-dependent cytotoxicity of GSK101 with  
300 extended explant culture at concentrations above 10nM (Fig. S7). Low concentrations of  
301 GSK101 elicit multiple short peaks of Ca<sup>2+</sup> signalling, which is more physiological compared  
302 with the large, sustained peaks observed at higher concentrations which might explain this  
303 [42]. These observations suggest perhaps that only moderate, short-term modulation of  
304 TRPV4 will be chondroprotective.

305 Servin-Vences et al suggest TRPV4 mechanosensitivity is dependent upon the type of  
306 stimulus applied [6]. Our data supports this hypothesis, complete abolition of NO release in  
307 response to IL-1 $\beta$  was observed following application of cyclic tensile strain (Figure 1), while  
308 hypo-osmotic challenge merely attenuated the response (Figure 2) suggesting TRPV4  
309 activation may be regulated distinct mechanisms and to different extents. Vriens et al report  
310 that TRPV4 activation in response to cell swelling is dependent upon arachidonic acid  
311 release [43] whereas Servin-Vences et al suggest direct channel gating occurs in response  
312 to membrane deflection [6].

313 The mechanosensitive ion channel PIEZO1 reportedly induces TRPV4 channel opening [44].  
314 PIEZO1 is activated chondrocytes following injurious loading and is suggested to play a  
315 greater role in chondroprotection than TRPV4 [6, 45]. It is possible the more pronounced  
316 anti-inflammatory effects of cyclic tensile strain observed in this study are the result of further  
317 TRPV4 activation downstream of this channel, which could be explored in future studies.  
318 However, while activation of PIEZO1 reportedly influences ciliogenesis [46] studies in  
319 osteocytes indicate that it does not interact with TRPV4 in the cilium [47].

320 TRPV4 cilia localisation was observed with greater localisation evident at to the ciliary base  
321 (Fig. 3C). TRPV4 activation altered this distribution such that localisation to the base or tip of  
322 the axoneme was not significantly different indicative of altered protein trafficking/IFT (Fig.  
323 3C). TRPV4 activation is coupled with translocation of TRPV4 to plasma membrane [48], in  
324 this study we observed increased TRPV4 labelling in the ciliary membrane (Fig. 3AB).  
325 Chemical deletion of primary cilia with chloral hydrate fully abolishes Ca<sup>2+</sup> signalling in  
326 response to TRPV4 activation [18] thus increased ciliary TRPV4 may be important for  
327 signalling.

328 HDAC6 is enriched within primary cilia catalysing tubulin de-acetylation and polymerization  
329 to regulate cilia resorption [27-29]. In this study, mechanical, hypo-osmotic and  
330 pharmaceutical activation of TRPV4 blocked cilia elongation in response to IL-1 $\beta$ . IFT and

331 cilia elongation is required for IL-1 $\beta$  mediated inflammatory signalling and downstream NF-  
332  $\kappa$ B signalling [5, 23, 24], therefore we suggest the anti-inflammatory effects of TRPV4  
333 activation regulate IFT and associated signalling via HDAC6 dependent modulation of ciliary  
334 tubulin. Previous studies demonstrate that GSK101 activates Ca<sup>2+</sup> signalling in isolated  
335 chondrocytes [6, 17, 49], while GSK205 inhibits this response and blocks Ca<sup>2+</sup> signalling in  
336 response to mechanical or osmotic loading [18, 50, 51]. While Ca<sup>2+</sup> signalling was not  
337 assessed in the current study, we hypothesise that Ca<sup>2+</sup> levels may regulate HDAC activity  
338 through activation of upstream kinases such as Ca<sup>2+</sup>/Calmodulin dependent kinase (CaMK),  
339 protein kinase D (PKD) and Aurora A kinase-dependent (AURKA) [27-29, 52-55]. Studies  
340 suggest TRPV4 stimulation with GSK101 promotes ERK/MAPK signalling in lung epithelial  
341 cells and cancer cells [56] and PKC activity in endothelial cells [57] which phosphorylate  
342 HDAC6 resulting in increased deacetylation activity [58, 59]. Indeed, increased HDAC6  
343 activity was observed in response to GSK101 (Fig. 4D).

344 In conclusion, this study demonstrates a role for TRPV4 activation in the anti-inflammatory  
345 mechanism of loading. In addition to providing new mechanistic understanding of this  
346 pathway, this study identifies TRPV4 as a potential therapeutic target and demonstrates that  
347 pharmaceutical activation of this protein could regulate inflammation and other IFT-  
348 dependent pathways involved in cartilage disease.

### 349 **Acknowledgments**

350 We thank Dr Hannah Heywood for supplying the TRPV4 antagonist GSK205.

### 351 **Author contributions**

352 All authors aided in revising this manuscript for intellectual content and approved the final  
353 version to be published.

354 Study design: Su Fu, Clare L Thompson, Martin M Knight.

355 Data acquisition: Su Fu, Clare L Thompson, Sheetal Inamdar, Huan Meng

356 Data analysis and interpretation: Su Fu, Clare L Thompson, Sheetal Inamdar, Wen Wang,  
357 Himadri Gupta, Martin M Knight.

### 358 **Role of the funding source**

359 Su Fu and Huan Meng are funded by the China Scholarship Council for his PhD studies at  
360 Queen Mary University of London. Dr Clare Thompson is supported by a project grant from  
361 the UK Medical Research Council (No: MR/L002876/1, PI: Knight). Sheetal Inamdar is  
362 supported by a project grant from the Biotechnology and Biomedical Sciences Research  
363 Council (No: BB/R003610/1, PI: Gupta).

### 364 **Conflict of interest**

365 The authors have no competing interests.

### 366 **References**

- 367 1. Chen A, Gupte C, Akhtar K, Smith P, and Cobb J, The global economic cost of  
368 osteoarthritis: How the uk compares. *Arthritis*, 2012. 2012.
- 369 2. Knecht S, Vanwanseele B, and Stüssi E, A review on the mechanical quality of articular  
370 cartilage—implications for the diagnosis of osteoarthritis. *Clinical biomechanics*, 2006.  
371 21(10):999-1012.
- 372 3. Chowdhury TT, Bader DL, and Lee DA, Dynamic compression inhibits the synthesis of  
373 nitric oxide and pge(2) by il-1beta-stimulated chondrocytes cultured in agarose  
374 constructs. *Biochem Biophys Res Commun*, 2001. 285(5):1168-74.
- 375 4. Xu Z, Buckley MJ, Evans CH, and Agarwal S, Cyclic tensile strain acts as an antagonist of  
376 il-1 beta actions in chondrocytes. *J Immunol*, 2000. 165(1):453-60.
- 377 5. Fu S, Thompson CL, Ali A, Wang W, Chapple JP, Mitchison HM, et al., Mechanical  
378 loading inhibits cartilage inflammatory signalling via an hdac6 and ift-dependent  
379 mechanism regulating primary cilia elongation. *Osteoarthritis Cartilage*, 2019.  
380 27(7):1064-1074.
- 381 6. Servin-Vences MR, Moroni M, Lewin GR, and Poole K, Direct measurement of trpv4 and  
382 piezo1 activity reveals multiple mechanotransduction pathways in chondrocytes.  
383 *Elife*, 2017. 6.

- 384 7. O'Connor CJ, Leddy HA, Benefield HC, Liedtke WB, and Guilak F, Trpv4-mediated  
385 mechanotransduction regulates the metabolic response of chondrocytes to dynamic  
386 loading. *Proceedings of the National Academy of Sciences*, 2014. 111(4):1316-1321.
- 387 8. Köhler R and Hoyer J, *Role of trpv4 in the mechanotransduction of shear stress in endothelial cells,*  
388 *in Trp ion channel function in sensory transduction and cellular signaling cascades*. 2006, CRC  
389 Press. p. 396-407.
- 390 9. Corrigan MA, Johnson GP, Stavenschi E, Riffault M, Labour MN, and Hoey DA, Trpv4-  
391 mediates oscillatory fluid shear mechanotransduction in mesenchymal stem cells in  
392 part via the primary cilium. *Sci Rep*, 2018. 8(1):3824.
- 393 10. Nilius B and Voets T, The puzzle of trpv4 channelopathies. *EMBO reports*, 2013.  
394 14(2):152-163.
- 395 11. Clark AL, Votta BJ, Kumar S, Liedtke W, and Guilak F, Chondroprotective role of the  
396 osmotically sensitive ion channel transient receptor potential vanilloid 4: Age- and  
397 sex-dependent progression of osteoarthritis in trpv4-deficient mice. *Arthritis Rheum*,  
398 2010. 62(10):2973-83.
- 399 12. O'Connor CJ, Griffin TM, Liedtke W, and Guilak F, Increased susceptibility of trpv4-  
400 deficient mice to obesity and obesity-induced osteoarthritis with very high-fat diet.  
401 *Annals of the Rheumatic Diseases*, 2013. 72(2):300-304.
- 402 13. Hu F, Zhu W, and Wang L, Microrna-203 up-regulates nitric oxide expression in  
403 temporomandibular joint chondrocytes via targeting trpv4. *Archives of oral biology*,  
404 2013. 58(2):192-199.
- 405 14. Xu S, Liu B, Yin M, Koroleva M, Mastrangelo M, Ture S, et al., A novel trpv4-specific  
406 agonist inhibits monocyte adhesion and atherosclerosis. *Oncotarget*, 2016.  
407 7(25):37622.
- 408 15. Pairet N, Mang S, Fois G, Keck M, Kühnbach M, Gindele J, et al., Trpv4 inhibition  
409 attenuates stretch-induced inflammatory cellular responses and lung barrier  
410 dysfunction during mechanical ventilation. *PLoS One*, 2018. 13(4):e0196055.
- 411 16. Dalsgaard T, Sonkusare SK, Teuscher C, Poynter ME, and Nelson MT, Pharmacological  
412 inhibitors of trpv4 channels reduce cytokine production, restore endothelial function  
413 and increase survival in septic mice. *Sci Rep*, 2016. 6:33841.
- 414 17. Kanju P, Chen Y, Lee W, Yeo M, Lee SH, Romac J, et al., Small molecule dual-inhibitors  
415 of trpv4 and trpa1 for attenuation of inflammation and pain. *Sci Rep*, 2016. 6:26894.
- 416 18. Phan MN, Leddy HA, Votta BJ, Kumar S, Levy DS, Lipshutz DB, et al., Functional  
417 characterization of trpv4 as an osmotically sensitive ion channel in porcine articular  
418 chondrocytes. *Arthritis Rheum*, 2009. 60(10):3028-37.
- 419 19. Qin H, Burnette DT, Bae YK, Forscher P, Barr MM, and Rosenbaum JL, Intraflagellar  
420 transport is required for the vectorial movement of trpv channels in the ciliary  
421 membrane. *Curr Biol*, 2005. 15(18):1695-9.
- 422 20. Wann AK, Zuo N, Haycraft CJ, Jensen CG, Poole CA, McGlashan SR, et al., Primary  
423 cilia mediate mechanotransduction through control of atp-induced ca<sup>2+</sup> signaling in  
424 compressed chondrocytes. *FASEB J*, 2012. 26(4):1663-71.

- 425 21. Kaushik AP, Martin JA, Zhang Q, Sheffield VC, and Morcuende JA, Cartilage  
426 abnormalities associated with defects of chondrocytic primary cilia in bardet-biedl  
427 syndrome mutant mice. *J Orthop Res*, 2009. 27(8):1093-9.
- 428 22. McGlashan SR, Haycraft CJ, Jensen CG, Yoder BK, and Poole CA, Articular cartilage  
429 and growth plate defects are associated with chondrocyte cytoskeletal abnormalities  
430 in tg737orpk mice lacking the primary cilia protein polaris. *Matrix Biol*, 2007.  
431 26(4):234-46.
- 432 23. Wann AK, Chapple JP, and Knight MM, The primary cilium influences interleukin-1beta-  
433 induced nfkappab signalling by regulating ikk activity. *Cell Signal*, 2014. 26(8):1735-  
434 42.
- 435 24. Wann AK and Knight MM, Primary cilia elongation in response to interleukin-1 mediates  
436 the inflammatory response. *Cell Mol Life Sci*, 2012. 69(17):2967-77.
- 437 25. Wann AK, Thompson CL, Chapple JP, and Knight MM, Interleukin-1beta sequesters  
438 hypoxia inducible factor 2alpha to the primary cilium. *Cilia*, 2013. 2(1):17.
- 439 26. Dinsmore C and Reiter JF, Endothelial primary cilia inhibit atherosclerosis. *EMBO Rep*,  
440 2016. 17(2):156-66.
- 441 27. Matsuyama A, Shimazu T, Sumida Y, Saito A, Yoshimatsu Y, Seigneurin- Berny D, et  
442 al., In vivo destabilization of dynamic microtubules by hdac6- mediated  
443 deacetylation. *The EMBO journal*, 2002. 21(24):6820-6831.
- 444 28. Thompson C, Chapple J, and Knight M, Primary cilia disassembly down-regulates  
445 mechanosensitive hedgehog signalling: A feedback mechanism controlling adamts-5  
446 expression in chondrocytes. *Osteoarthritis and Cartilage*, 2014. 22(3):490-498.
- 447 29. Ran J, Yang Y, Li D, Liu M, and Zhou J, Deacetylation of  $\alpha$ -tubulin and cortactin is  
448 required for hdac6 to trigger ciliary disassembly. *Sci Rep*, 2015. 5:12917.
- 449 30. Reed NA, Cai D, Blasius TL, Jih GT, Meyhofer E, Gaertig J, et al., Microtubule  
450 acetylation promotes kinesin-1 binding and transport. *Curr Biol*, 2006. 16(21):2166-  
451 72.
- 452 31. Dompierre JP, Godin JD, Charrin BC, Cordelieres FP, King SJ, Humbert S, et al.,  
453 Histone deacetylase 6 inhibition compensates for the transport deficit in huntington's  
454 disease by increasing tubulin acetylation. *J Neurosci*, 2007. 27(13):3571-83.
- 455 32. Thompson CL, Yasmin H, Varone A, Wiles A, Poole CA, and Knight MM, Lithium chloride  
456 prevents interleukin-1beta induced cartilage degradation and loss of mechanical  
457 properties. *J Orthop Res*, 2015. 33(10):1552-9.
- 458 33. Tanaka R, Muraki K, Ohya S, Yamamura H, Hatano N, Itoh Y, et al., Trpv4-like non-  
459 selective cation currents in cultured aortic myocytes. *Journal of pharmacological  
460 sciences*, 2008. 108(2):179-189.
- 461 34. Güler AD, Lee H, Iida T, Shimizu I, Tominaga M, and Caterina M, Heat-evoked activation  
462 of the ion channel, trpv4. *Journal of Neuroscience*, 2002. 22(15):6408-6414.
- 463 35. Becker D, Blase C, Bereiter-Hahn J, and Jendrach M, Trpv4 exhibits a functional role in  
464 cell-volume regulation. *Journal of Cell Science*, 2005. 118(11):2435-2440.

- 465 36. Walter B, Purmessur D, Moon A, Occhiogrosso J, Laudier D, Hecht A, et al., Reduced  
466 tissue osmolarity increases trpv4 expression and pro-inflammatory cytokines in  
467 intervertebral disc cells. *Eur Cell Mater*, 2016. 32:123.
- 468 37. Henry CO, Dalloneau E, Pérez-Berezo M-T, Plata C, Wu Y, Guillon A, et al., In vitro and  
469 in vivo evidence for an inflammatory role of the calcium channel trpv4 in lung  
470 epithelium: Potential involvement in cystic fibrosis. *American Journal of Physiology-  
471 Lung Cellular and Molecular Physiology*, 2016. 311(3):L664-L675.
- 472 38. Balakrishna S, Song W, Achanta S, Doran SF, Liu B, Kaelberer MM, et al., Trpv4  
473 inhibition counteracts edema and inflammation and improves pulmonary function and  
474 oxygen saturation in chemically induced acute lung injury. *American Journal of  
475 Physiology-Lung Cellular and Molecular Physiology*, 2014. 307(2):L158-L172.
- 476 39. Okada Y, Shirai K, Miyajima M, Reinach PS, Yamanaka O, Sumioka T, et al., Loss of  
477 trpv4 function suppresses inflammatory fibrosis induced by alkali-burning mouse  
478 corneas. *PLoS One*, 2016. 11(12):e0167200.
- 479 40. Grace MS, Bonvini SJ, Belvisi MG, and McIntyre P, Modulation of the trpv4 ion channel  
480 as a therapeutic target for disease. *Pharmacology & therapeutics*, 2017. 177:9-22.
- 481 41. Hubert A, Cauliez B, Chedeville A, Husson A, and Lavoine A, Osmotic stress, a  
482 proinflammatory signal in caco-2 cells. *Biochimie*, 2004. 86(8):533-541.
- 483 42. Gilchrist CL, Leddy HA, Kaye L, Case ND, Rothenberg KE, Little D, et al., Trpv4-  
484 mediated calcium signaling in mesenchymal stem cells regulates aligned collagen  
485 matrix formation and vinculin tension. *Proceedings of the National Academy of  
486 Sciences*, 2019. 116(6):1992-1997.
- 487 43. Vriens J, Watanabe H, Janssens A, Droogmans G, Voets T, and Nilius B, Cell swelling,  
488 heat, and chemical agonists use distinct pathways for the activation of the cation  
489 channel trpv4. *Proc Natl Acad Sci U S A*, 2004. 101(1):396-401.
- 490 44. Swain SM, Romac JM, Shahid RA, Pandol SJ, Liedtke W, Vigna SR, et al., Trpv4  
491 channel opening mediates pressure-induced pancreatitis initiated by piezo1  
492 activation. *J Clin Invest*, 2020. 130(5):2527-2541.
- 493 45. Lee W, Leddy HA, Chen Y, Lee SH, Zelenski NA, McNulty AL, et al., Synergy between  
494 piezo1 and piezo2 channels confers high-strain mechanosensitivity to articular  
495 cartilage. *Proc Natl Acad Sci U S A*, 2014. 111(47):E5114-22.
- 496 46. Miyazaki A, Sugimoto A, Yoshizaki K, Kawarabayashi K, Iwata K, Kurogoushi R, et al.,  
497 Coordination of wnt signaling and ciliogenesis during odontogenesis by piezo type  
498 mechanosensitive ion channel component 1. *Sci Rep*, 2019. 9(1):14762.
- 499 47. Lee KL, Guevarra MD, Nguyen AM, Chua MC, Wang Y, and Jacobs CR, The primary  
500 cilium functions as a mechanical and calcium signaling nexus. *Cilia*, 2015. 4:7.
- 501 48. Cayouette S and Boulay G, Intracellular trafficking of trp channels. *Cell Calcium*, 2007.  
502 42(2):225-232.
- 503 49. Hurd L, Kirwin SM, Boggs M, Mackenzie WG, Bober MB, Funanage VL, et al., A mutation  
504 in trpv4 results in altered chondrocyte calcium signaling in severe metatropic  
505 dysplasia. *Am J Med Genet A*, 2015. 167A(10):2286-93.



- 506 50. Yu SM, Kim HA, and Kim SJ, 2-deoxy-d-glucose regulates dedifferentiation through beta-  
507 catenin pathway in rabbit articular chondrocytes. *Exp Mol Med*, 2010. 42(7):503-13.
- 508 51. O'Connor CJ, Leddy HA, Benefield HC, Liedtke WB, and Guilak F, Trpv4-mediated  
509 mechanotransduction regulates the metabolic response of chondrocytes to dynamic  
510 loading. *Proc Natl Acad Sci U S A*, 2014. 111(4):1316-21.
- 511 52. Youn H-D, Grozinger CM, and Liu JO, Calcium regulates transcriptional repression of  
512 myocyte enhancer factor 2 by histone deacetylase 4. *Journal of Biological Chemistry*,  
513 2000. 275(29):22563-22567.
- 514 53. McKinsey TA, Zhang CL, and Olson EN, Activation of the myocyte enhancer factor-2  
515 transcription factor by calcium/calmodulin-dependent protein kinase-stimulated  
516 binding of 14-3-3 to histone deacetylase 5. *Proceedings of the National Academy of  
517 Sciences*, 2000. 97(26):14400-14405.
- 518 54. Karppinen S, Hänninen SL, Rapila R, and Tavi P, Sarcoplasmic reticulum ca<sup>2+</sup>-induced  
519 ca<sup>2+</sup> release regulates class iia hdac localization in mouse embryonic  
520 cardiomyocytes. *Physiological reports*, 2018. 6(2).
- 521 55. Pugacheva EN, Jablonski SA, Hartman TR, Henske EP, and Golemis EA, Hef1-  
522 dependent aurora a activation induces disassembly of the primary cilium. *Cell*, 2007.  
523 129(7):1351-63.
- 524 56. Nayak PS, Wang Y, Najrana T, Priolo LM, Rios M, Shaw SK, et al., Mechanotransduction  
525 via trpv4 regulates inflammation and differentiation in fetal mouse distal lung  
526 epithelial cells. *Respiratory research*, 2015. 16(1):60.
- 527 57. Baratchi S, Keov P, Darby WG, Lai A, Khoshmanesh K, Thurgood P, et al., The trpv4  
528 agonist gsk1016790a regulates the membrane expression of trpv4 channels.  
529 *Frontiers in pharmacology*, 2019. 10.
- 530 58. Du Y, Seibenhener ML, Yan J, Jiang J, and Wooten MC, Apkc phosphorylation of hdac6  
531 results in increased deacetylation activity. *PLoS One*, 2015. 10(4):e0123191.
- 532 59. Williams KA, Zhang M, Xiang S, Hu C, Wu J-Y, Zhang S, et al., Extracellular signal-  
533 regulated kinase (erk) phosphorylates histone deacetylase 6 (hdac6) at serine 1035  
534 to stimulate cell migration. *Journal of Biological Chemistry*, 2013. 288(46):33156-  
535 33170.

## Figure legends

### **Figure 1. Cyclic tensile strain inhibits IL-1 $\beta$ mediated NO and PGE<sub>2</sub> release via a TRPV4 dependent pathway in isolated chondrocytes.**

The TRPV4 antagonist, GSK205 (10  $\mu$ M), abolishes the anti-inflammatory effects of mechanical loading (CTS, 10%, 0.33 Hz) at 1 ng/ml IL-1 $\beta$  on (A) nitrite and (B) PGE<sub>2</sub> release at 24 h. Data represents mean  $\pm$  SD for n=6 wells per group using cells isolated from 2 different donors. Statistics: Three-way ANOVA and post hoc Tukey's test. # represents statistically significant difference between IL-1 $\beta$  treated and corresponding untreated cells.

### **Figure 2. Hypo-osmotic challenge inhibits IL-1 $\beta$ mediated NO release via a TRPV4 dependent pathway in isolated chondrocytes and cartilage explants**

The TRPV4 antagonist, GSK205, suppresses the anti-inflammatory effects of hypo- osmotic challenge. Nitrite levels measured in the media for (A) isolated cells and (C) cartilage explants in hypo- or iso-osmotic media. Chondrocytes and cartilage explants were treated with and without IL-1 $\beta$  (1 ng/ml) for 24 h and 12 d respectively with and without the TRPV4 inhibitor GSK205 (10  $\mu$ M). Hypo-osmotic challenge had no effect on cell viability as determined by (B) bright field images of isolated chondrocytes (D) confocal microscopy of explants stained with Calcein-AM (live cells, green) and ethidium homodimer (dead cells, red). Scale bar represents 100  $\mu$ m. Data represents mean  $\pm$  SD for n=6 separate wells (A) or n=8 separate explants (C) using cells/explants isolated from 2 different donors. Statistics: Three-way ANOVA and post hoc Tukey's test. # represents statistically significant difference between IL-1 $\beta$  treated and corresponding untreated cells.

### **Figure 3. TRPV4 activation increases cilia expression of TRPV4 and inhibits cilia elongation in response to IL-1 $\beta$**

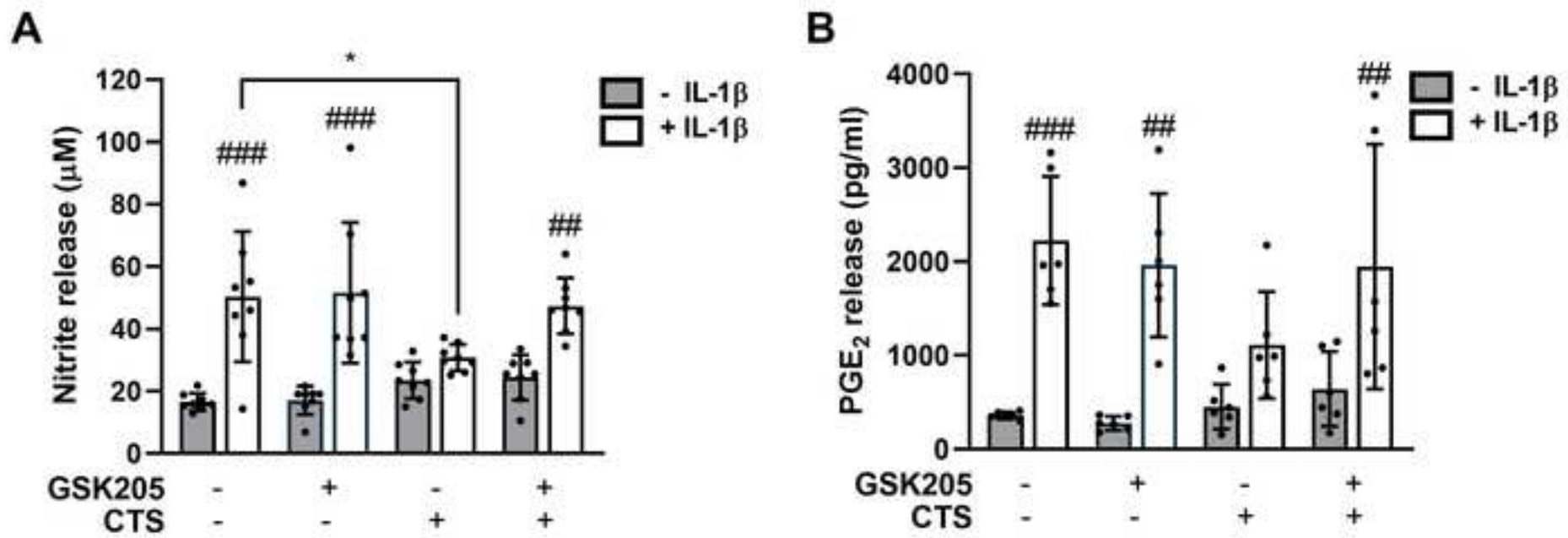
Primary articular chondrocytes were subjected to mechanical loading (CTS, 10%, 0.33 Hz), hypo-osmotic challenge (200 mOsm) or the TRPV4 agonist 1 nM GSK101 for 24 h. (A) Representative maximum intensity projection of confocal images showing co-localisation of Acet- $\alpha$ -tubulin (Red) and TRPV4 (Green). Scale bar represents 1  $\mu$ m. Pharmaceutical activation of TRPV4 increased the (B) mean intensity of TRPV4 labelling on primary cilia (n=20-30 cilia) and (C) altered the distribution of TRPV4 on the cilium (n=20-30 cilia). (D) Representative maximum intensity projection confocal microscopy images of isolated chondrocytes treated with  $\pm$  1 ng/ml IL-1 $\beta$   $\pm$  1 nM GSK101 then labelled for acetylated  $\alpha$ -tubulin (red) and counter stained with DAPI (blue). Scale bar represents 10  $\mu$ m. (E) Primary cilia length and (F) associated % elongation were measured at 24 h. % cilia elongation results showing IL-1 $\beta$  induced change in cilia length for cells cultured (G) with and without mechanical loading and in (H) iso- and hypo-osmotic media. For % cilia elongation, data represents cilia length change in the presence of IL-1 $\beta$  (1 ng/ml, 24 h) normalised to median values in corresponding condition without IL-1 $\beta$ . Box plots are displayed as median, with error bars depicting min/max values (for E-H, n=70-130 cilia). Statistics: One-way ANOVA (B) and Two-way ANOVA (D, E, G and H) with post hoc Tukey's test and T-test (C, F).

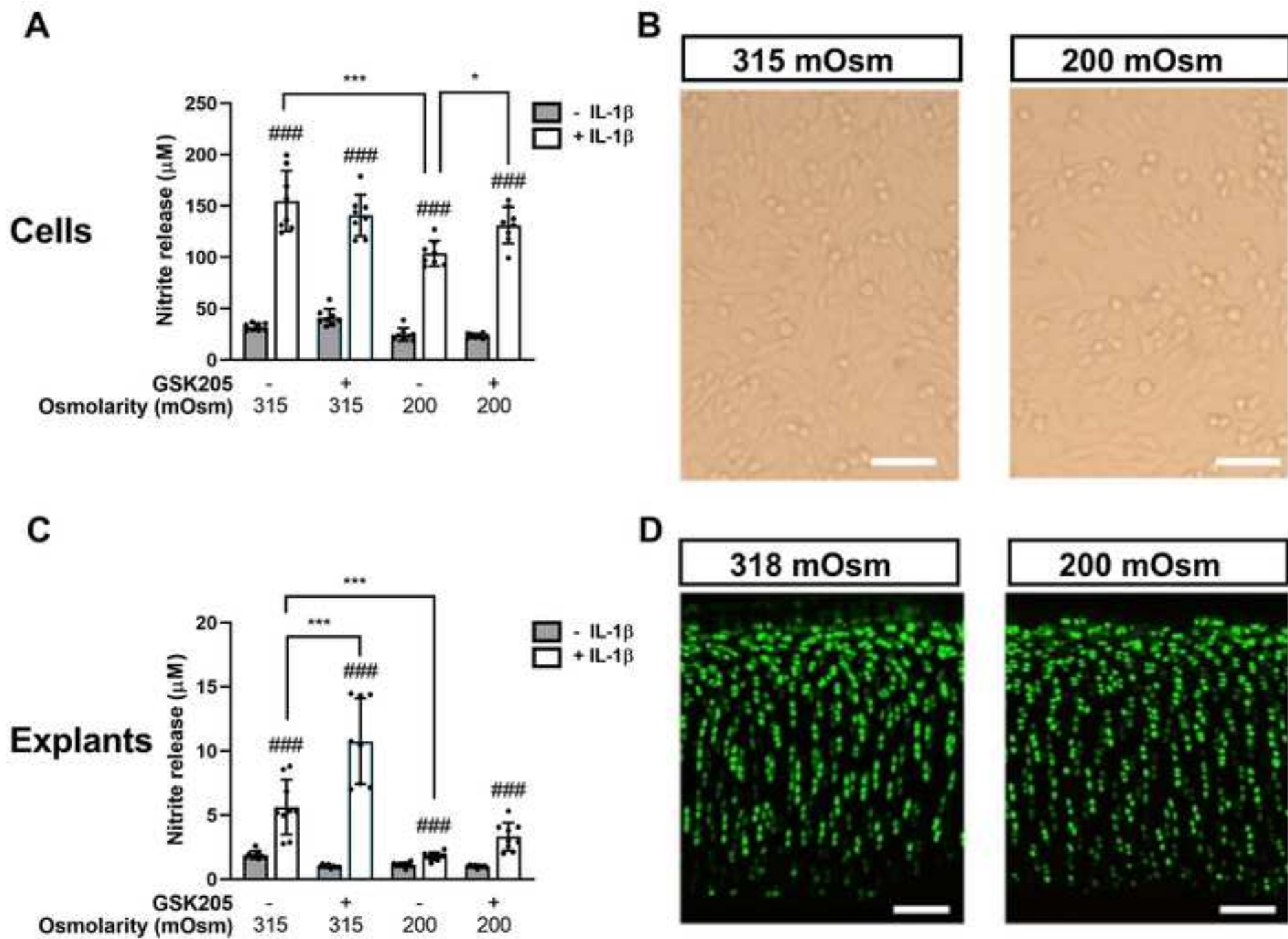
#### **Figure 4. TRPV4 activation abolishes IL-1 $\beta$ inflammatory signalling via HDAC6 activation**

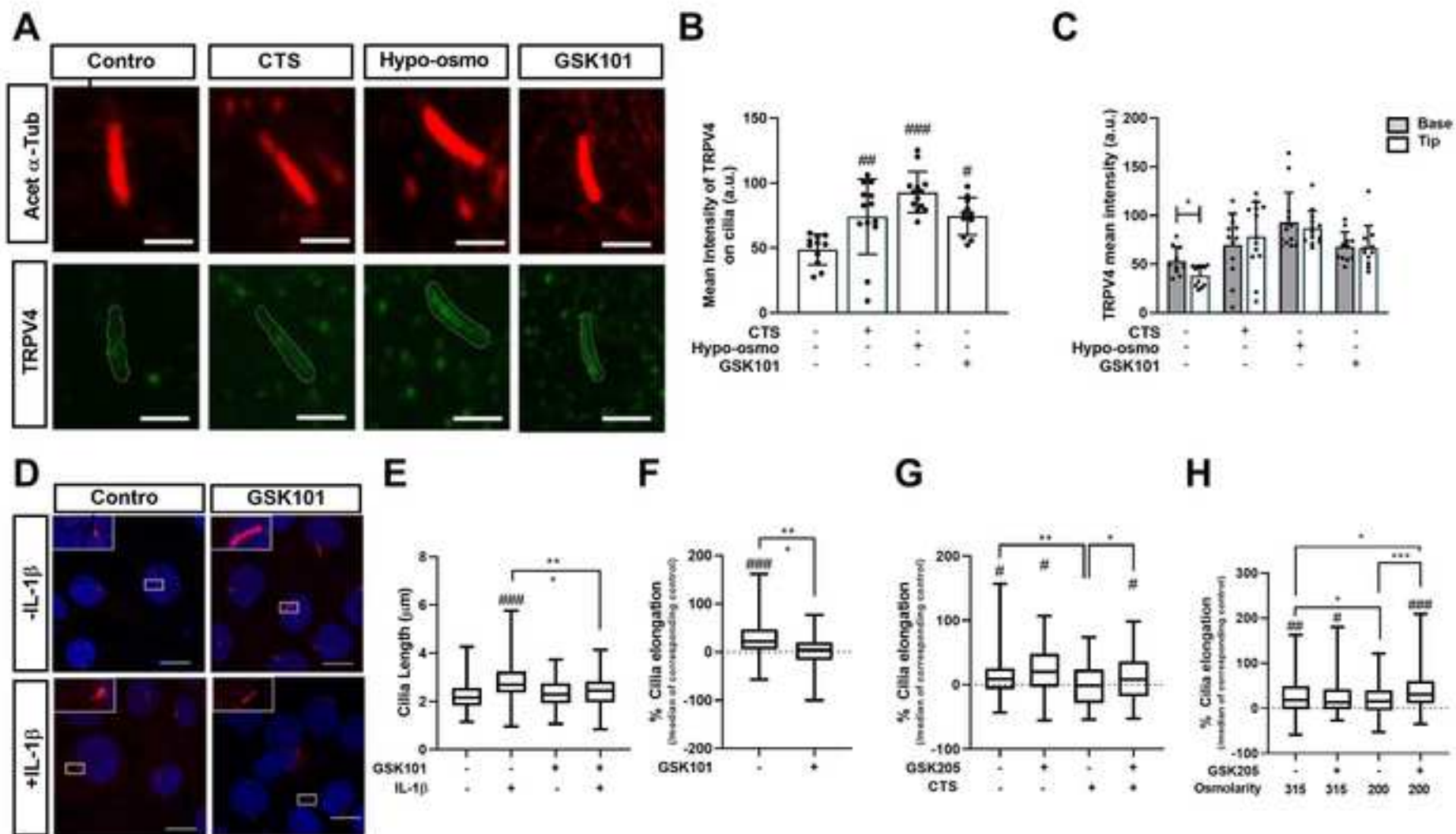
Levels of (A) nitrite (B) PGE<sub>2</sub> and (C) COX-2 expression associated with isolated chondrocytes  $\pm$ IL-1 $\beta$  (1 ng/ml) in the presence or absence of GSK101 for 24 hrs. GSK101 promotes (D) HDAC6 activity, induces the (E) de-acetylation and (E) de-polymerization of  $\alpha$ -tubulin, as measured by western blot of acetylated  $\alpha$ -tubulin (Acet  $\alpha$ -Tub),  $\alpha$ -tubulin ( $\alpha$ -Tub) and non-polymerized  $\alpha$ -tubulin. Full western blots can be found in supplementary figure S9. (G) HDAC6 inhibition with tubacin (500 nM) abolished the anti-inflammatory effect of GSK101 on NO release. Data represents mean  $\pm$  SD for n=6 (A, B, D and G) and n=4 (C, E and F) Statistics: Two-way ANOVA and post hoc Tukey's test (A-C), T-test (D-G). # represents statistically significant difference between IL-1 $\beta$  treated and corresponding untreated cells.

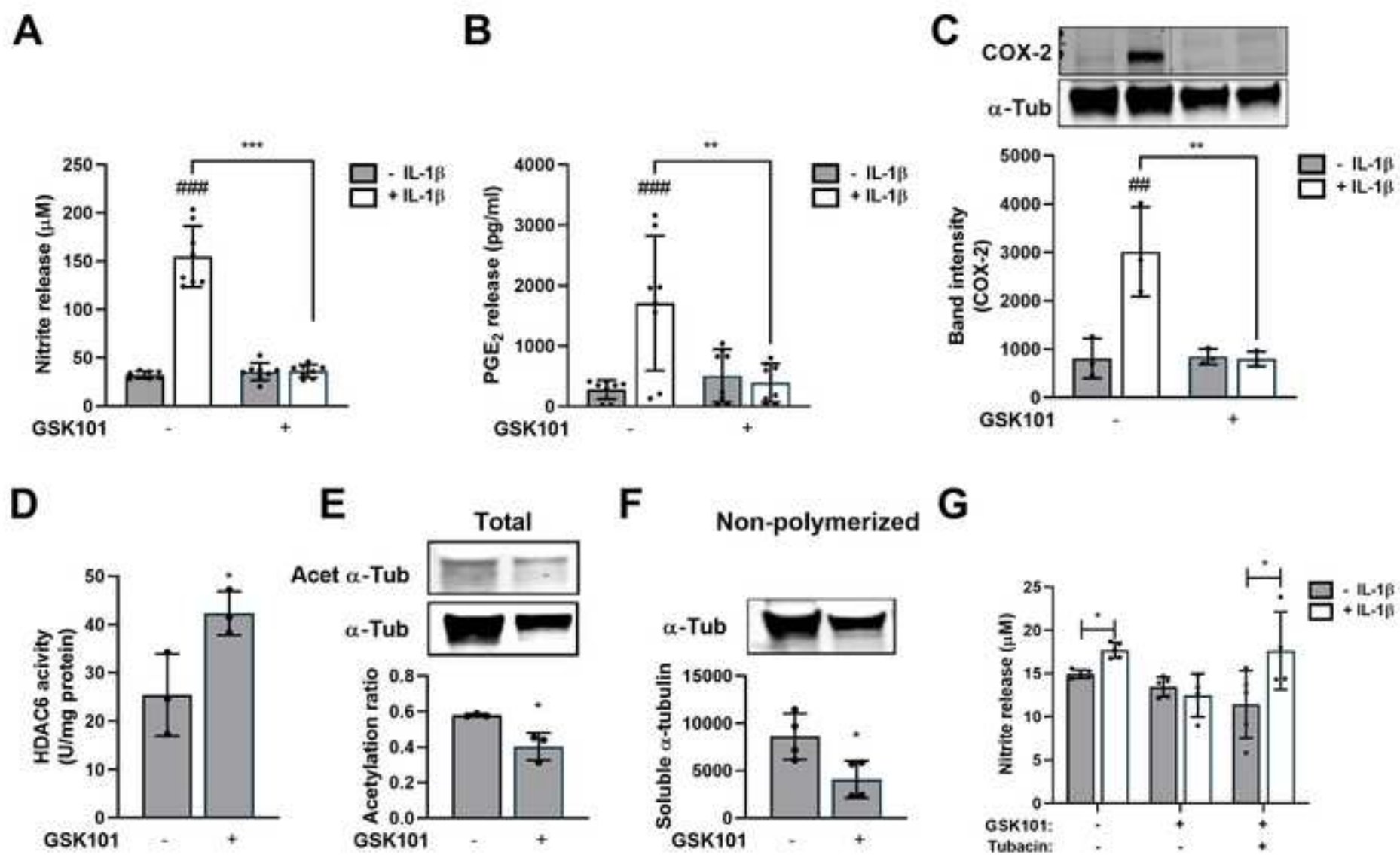
#### **Figure 5. TRPV4 activation suppresses IL-1 $\beta$ induced NO release, matrix degradation and loss of mechanical properties in cartilage explants.**

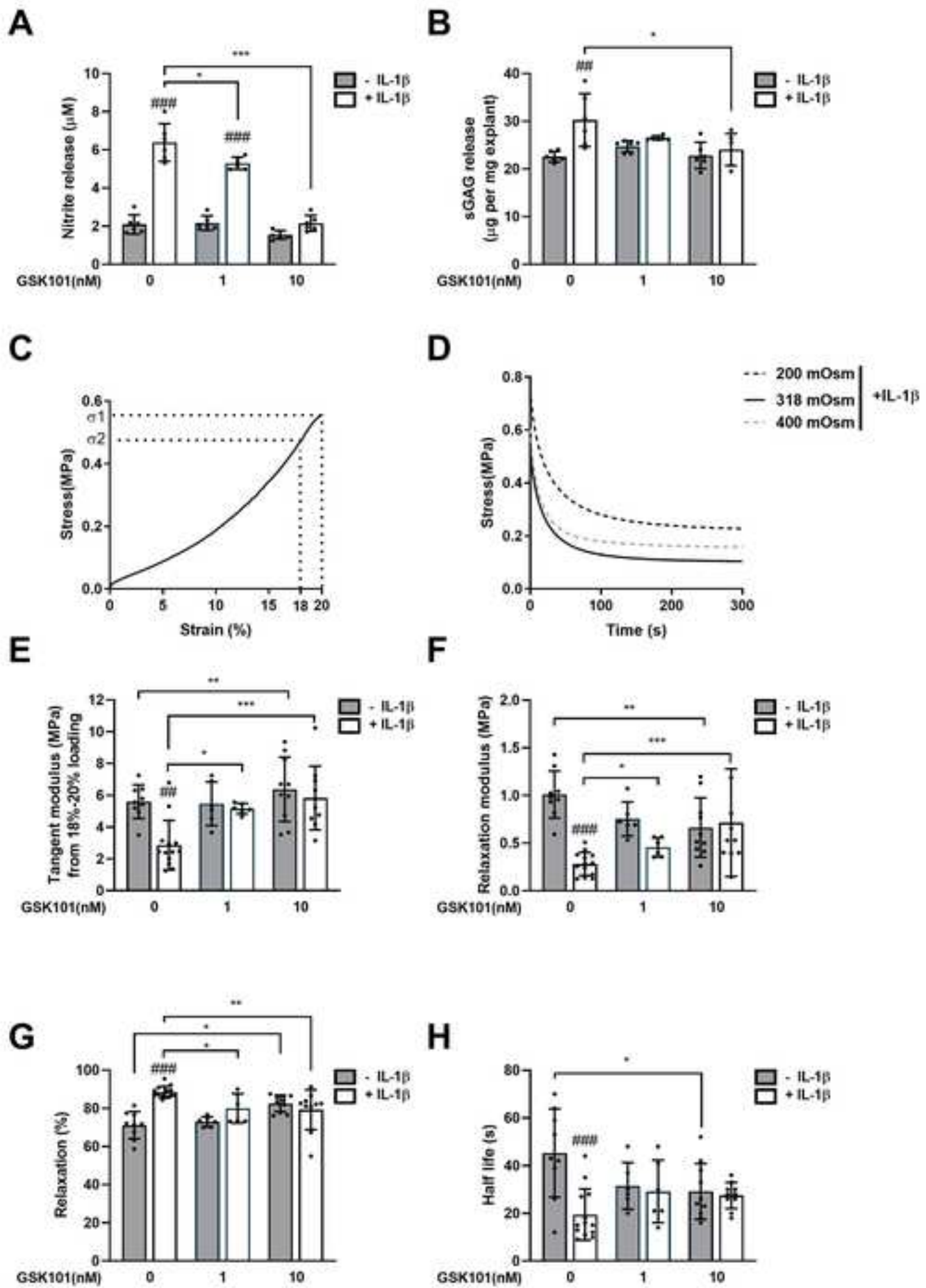
Full-depth cartilage explants were treated with the TRPV4 agonist GSK101 (0, 1, 10 nM) in the presence or absence of 1 ng/ml IL-1 $\beta$  for 12 d. The nitrite (A) and sGAG (B) content of the culture media was measured and normalised to wet weight. Cartilage explants were compressed to obtain the stress-strain (C) and stress-relaxation (D) plots, for the calculation of cartilage mechanical properties. The responding mechanical properties of tangent modulus from 18-20% compression (E), relaxation modulus (F), percentage relaxation (G) and half-life (H). Data represents mean  $\pm$  SD, n=6-12 explants from 4 different donors. Statistics: Two-way ANOVA with post hoc Tukey's test. # represents statistically significant difference between IL-1 $\beta$  treated and corresponding untreated cells.















Click here to access/download  
**Supplemental Material**  
Supplementary figures\_resub.docx



## 1 **Introduction**

2 Osteoarthritis (OA) affects over 4.4 million people in the UK alone representing significant  
3 economic cost [1]. Cartilage health is maintained in response to mechanical stimuli, articular  
4 cartilage is routinely exposed to a wide array of dynamic mechanical loading consisting of  
5 compressive, shear and tensile strains as well as associated alterations in fluid shear and  
6 osmolality [2]. Mechanical loading in the form of compression or tensile strain is anti-  
7 inflammatory in chondrocytes and blocks the release of the pro-inflammatory mediator's  
8 nitric oxide (NO) and prostaglandin E<sub>2</sub> (PGE<sub>2</sub>) in response to interleukin-1 $\beta$  (IL-1 $\beta$ ) [3-5].  
9 Inflammatory signalling contributes to cartilage degradation in OA thus understanding the  
10 link between mechanical loading and inflammation will have significant therapeutic impact.

11 The osmotic-sensitive Ca<sup>2+</sup> ion channel Transient Receptor Potential Vanilloid 4 (TRPV4) is  
12 highly expressed in articular chondrocytes and is activated by mechanical stimuli [6, 7].  
13 TRPV4 is required for mechanotransduction in chondrocytes and other cells types [7-9]. It  
14 mediates the regulation of pro-anabolic and anti-catabolic genes promoting matrix  
15 production and accumulation in agarose-embedded chondrocytes [7, 9]. TRPV4 mutations  
16 result in human skeletal dysplasia suggesting a role in bone development (for review see  
17 [10]). Indeed, chondrocytes from TRPV4<sup>-/-</sup> mice exhibit loss of osmosensitivity accompanied  
18 by joint degeneration indicating a central role for this channel protein in maintaining joint  
19 homeostasis [11, 12]. Pharmaceutical activation of TRPV4 inhibits NO release in response  
20 to inflammatory cytokines suggesting a potential mechanistic role in the anti-inflammatory  
21 effects of mechanical loading [13, 14]. However, in apparent contradiction of these findings  
22 TRPV4 inhibition exerts an anti-inflammatory effect in the cardiovascular system, lung and  
23 peripheral nervous system [15-17]. This study therefore aims to clarify the regulatory role of  
24 TRPV4 in cartilage inflammatory signalling.

25 TRPV4 localises to the plasma membrane and primary cilium, a small microtubule based  
26 signalling compartment present at the cell surface [18, 19]. Primary cilia have been

27 implicated in both chondrocyte mechanotransduction [20-22] and inflammatory signalling  
28 [23-26]. The cytoplasmic tubulin deacetylase histone deacetylase 6 (HDAC6) is enriched  
29 within the cilium and modulates cilia resorption through de-acetylation and polymerization of  
30 ciliary tubulin [27-29]. Post translational modification of ciliary tubulin influences intraflagellar  
31 transport (IFT), the microtubule based motility present within the cilium required for cilia-  
32 mediated signalling [30, 31]. Previously we report that mechanical loading counteracts  
33 inflammatory signalling in response to the pro-inflammatory cytokine interleukin 1 $\beta$  (IL-1 $\beta$ )  
34 via HDAC6 activation in association with alterations in IFT/cilia [5]. A role for TRPV4 in this  
35 pathway has not previously been identified.

36 In the present study, we demonstrate for the first time that TRPV4 activation by cyclic tensile  
37 strain, hypo-osmotic challenge or the TRPV4 agonist GSK1016790A inhibits pro-  
38 inflammatory IL-1 $\beta$  signalling and cartilage degradation associated with alterations in primary  
39 cilia elongation. TRPV4 may therefore provide a novel target for the treatment of joint  
40 disease and other inflammatory pathologies.

## 41 **Methods**

### 42 **Antibodies and reagents**

43 Chondrocytes were treated with interleukin-1 $\beta$  (IL-1 $\beta$ , 200-01B; Peprotech, London, UK),  
44 TRPV4 antagonist GSK205 (616522; Merck Millipore, London, UK) and agonist  
45 GSK1016790A (GSK101, G0798; Sigma Aldrich, Poole, UK). Antibodies for  
46 immunocytochemistry: acetylated  $\alpha$ -tubulin (1:2000, T7451, Sigma Aldrich, Poole, UK) and  
47 TRPV4 (1:200, SAB2104243, Sigma Aldrich). Nuclei were counterstained with 4',6-  
48 diamidino-2-phenylindole (DAPI, Sigma Aldrich). Antibodies for western blotting: acetylated  
49  $\alpha$ -tubulin (1:1000, T7451, Sigma Aldrich) and  $\alpha$ -tubulin (1:1000, ab4074, Abcam, Cambridge,  
50 UK).

### 51 **Cartilage explant and chondrocyte culture**

52 Bovine cartilage explants and chondrocytes were obtained from 16 month steers as  
53 previously described [28]. Full depth articular cartilage was removed from the proximal  
54 surface of the metacarpal phalangeal joint and chondrocytes isolated by enzymatic  
55 digestion. Explants were harvested using a 5 mm diameter biopsy punch (BP-50F, Selles  
56 Medical Ltd, UK). Both were cultured at 37 °C, 5% CO<sub>2</sub> in Dulbeccos Minimal Essential  
57 Medial (DMEM, D5921, Sigma-Aldrich, Poole, UK) supplemented with 10% (v/v) foetal calf  
58 serum (FCS, F7524, Gibco, Paisley, UK), 1.9 mM L-glutamine (G7513), 96 U/ml penicillin  
59 (P4333, All Sigma-Aldrich, Poole, UK). Explants were rested for 2 d prior to experimentation  
60 while isolated chondrocytes were cultured to confluence.

### 61 **Application of cyclic tensile strain**

62 Isolated chondrocytes were cultured on collagen coated flexible elastomeric membranes and  
63 subjected to uniform, equibiaxial cyclic tensile strain (CTS) applied using the Flexcell 5000T  
64 system (Dunn Labortechnik GmbH). Cells were subjected to 0-10% strain for 24 h at 0.33 Hz.

### 65 **Application of osmotic loading**

66 Isolated cells were cultured for 24 h without serum in osmotically adjusted media at 200, 315  
67 or 400 mOsm, hereafter referred as hypo-, iso- or hyper- osmotic media respectively.  
68 Explants were cultured for up to 12 d under similar conditions with the addition of serum to  
69 maintain chondrocyte viability resulting in a slightly higher osmolarity of 318 mOsm for the  
70 iso-osmotic media. The osmolarity of all solutions was adjusted by adding D-mannitol  
71 (M4125, Sigma-Aldrich) or distilled water and measured using a freezing point depression  
72 osmometer.

### 73 **Biochemical analysis of NO, PGE<sub>2</sub> and sGAG release**

74 Nitric Oxide (NO) release was assessed using the Griess assay based on quantification of  
75 nitrite (NO<sub>2</sub>), the stable product of NO degradation. Nitrite content was quantified against a  
76 sodium nitrite standard curve using the Galaxy Fluorstar spectrophotometer (BMG Labtech,

77 UK). An immunoassay kit (KGE004B, R&D Systems, UK) was used to quantify PGE<sub>2</sub>  
78 concentrations in the media according to the manufacturer's instructions. Results were  
79 corrected for non-specific binding and calibrated using a PGE<sub>2</sub> standard curve. The release  
80 of sGAG into the culture media was quantified using the dimethylmethyleneblue (DMMB)  
81 assay against a chondroitin sulphate standard curve (6-sulphate:4-sulphate; 0.33:1; Sigma–  
82 Aldrich).

### 83 **Immunocytochemistry, live imaging and confocal microscopy**

84 For immunocytochemistry, samples were fixed with 4% paraformaldehyde for 10 min,  
85 permeabilised for 5 min with 0.5% triton-X100/phosphate buffered saline (PBS) then blocked  
86 with 5% goat serum/PBS for 1 h. Primary antibody was incubated at 4°C overnight followed  
87 by appropriate Alexa Fluor conjugated secondary antibodies (Molecular Probes) for 1 h at  
88 room temperature. Cells were counterstained with 1 µg/ml DAPI for 5 min. **For live imaging,**  
89 **cell viability was assessed by live/dead staining. Explants were incubated for 30 min with 5**  
90 **µM Calcein AM and 5 µM Ethidium homodimer-1 (EthD-1) prepared in appropriate osmotic**  
91 **adjusted media, washed and immediately imaged. Samples were imaged using a Zeiss 710**  
92 **ELYRA PS.1 microscope. For cilia analysis, samples were imaged using an x63/1.4 NA**  
93 **objective to generate confocal z-sections made throughout the cell depth (approximately 20**  
94 **sections) using 0.25 µm step size with an image format of 1024 x 1024 yielding a pixel size**  
95 **of 0.13 x 0.13 µm (image size approximately 135 x 135 µm). Cilia length and prevalence was**  
96 **quantified from resulting maximum projection images using Image J software (National**  
97 **Institutes of Health, Maryland, USA).**

### 98 **Western blotting**

99 Cells were lysed in RIPA buffer (R0278, Sigma Aldrich) and total protein quantified by  
100 Bicinchoninic acid (BCA) assay. For the fractionation of soluble and polymerized tubulin,  
101 extraction buffer A (137 mM NaCl, 20 mM Tris-HCl, 1% Triton X-100, and 10% glycerol) was  
102 added to cells at 4 °C for 3 min, plates were gently swirled and the buffer removed and

103 saved as the soluble tubulin fraction. Immediately after, extraction buffer B (buffer A + 1%  
104 SDS) was added for 1 min, the remaining sample was scraped, incubated on ice for 30 min  
105 and saved as the polymerized tubulin fraction.

106 SDS-PAGE was performed under reducing conditions and proteins transferred to  
107 nitrocellulose membranes. Membranes were blocked in odyssey blocking buffer (Li-Cor  
108 Cambridge, UK) prior to overnight incubation with primary antibodies and infrared secondary  
109 antibodies (Li-Cor). Proteins were visualized using the Li-Cor Odyssey and quantified using  
110 Image Studio Lite software (Li-Cor).

### 111 **HDAC6 activity measurement**

112 A commercial fluorometric assay kit (K466-100, Biovision) was used to measure HDAC6  
113 activity according to the manufacturer's instructions. This assay determines enzyme activity  
114 by exploiting the selectivity of tubacin for HDAC6 in combination with a fluorescent synthetic  
115 acetylated-peptide substrate. Cultures were lysed, a 10 µl aliquot was mixed with either  
116 acetylated substrate (sample) or with 2 µM tubacin and acetylated substrate (inhibitor  
117 control) then incubated for 30 min at 37°C. The deacetylase-dependent release of a 7-  
118 amino-4-trifluoromethylcoumarin fluorophore (excitation/emission at 350/490 nm) was then  
119 measured on a Galaxy Fluorstar spectrophotometer (BMG Labtech, UK) and HDAC6 activity  
120 calculated as [sample-inhibitor control].

### 121 **Mechanical testing of cartilage explants**

122 The mechanical behaviour of individual cartilage explants was measured using an MTS,  
123 Bionix 100. A 2 mm diameter core was cut from the centre of each 5 mm diameter cartilage  
124 explant and a tare load of 0.01 N applied to each explant which was then hydrated in culture  
125 media. The explants were subjected to a 20% uniaxial unconfined compressive strain (20%  
126 /min). This was followed by a stress relaxation period at constant 20% strain in which the  
127 load was recorded for a further 300 s. The load was recorded throughout the test at a

128 sampling frequency of 60 Hz. Stress–strain and stress–time curves were generated for each  
129 specimen and the following mechanical properties of the cartilage determined:

130 Tangent Modulus (MPa) =  $\frac{\sigma_{\varepsilon=0.2} - \sigma_{\varepsilon=0.18}}{0.02}$

131 Relaxation Modulus (MPa) =  $\frac{\sigma_{t=300s}}{0.2}$

132 Percentage Relaxation (%) =  $\frac{\sigma_{t=0s} - \sigma_{t=300s}}{\sigma_{t=0s}}$

133 The relaxation half-life was calculated as the time from the start of the relaxation phase until  
134 stress reduced to half the peak value.

### 135 **Statistical analyses**

136 The sample size for each experiment was chosen based on previous studies [5, 32] where  
137 analysis of cartilage degradation by biochemistry, immunohistochemistry and mechanical  
138 testing demonstrated that 6-8 samples/group is sufficient to detect a 25% difference in  
139 cartilage matrix catabolism at 80% power and a significance of  $p < 0.05$ . Data analysis was  
140 conducted using GraphPad Prism version 8 (GraphPad software, La Jolla California USA,  
141 [www.graphpad.com](http://www.graphpad.com)). Normality testing (Kolmogorov Smirnov test) was performed to confirm  
142 that data exhibited Gaussian distribution. For data sets that were not normally distributed,  
143 namely cilia length data, Box Cox transformation ( $\lambda=0.5$ ) was performed prior to statistical  
144 analyses. Statistical significance was determined by T-Test, One-way, Two-way or Three-  
145 way ANOVA as appropriate with post-hoc Tukey's multiple comparisons performed to  
146 identify significant differences between groups. Statistically significant differences were  
147 determined based on a threshold of \* =  $p < 0.05$ , \*\* =  $p < 0.01$  and \*\*\* =  $p = 0.001$ . Data is  
148 presented as mean  $\pm$  standard deviation (SD) unless otherwise stated.

149 **Results**

150 **TRPV4 activation is required for the anti-inflammatory effects of mechanical loading**  
151 **in isolated chondrocytes**

152 IL-1 $\beta$  treatment (24 h) resulted in significant, dose-dependent release of NO and PGE<sub>2</sub> (Fig.  
153 1AB, S1AB). In response to 1 ng/ml IL-1 $\beta$  isolated chondrocytes exhibited a 3.04-fold  
154 increase in nitrite levels indicative of NO release (Fig. 1A), and a 4.84-fold increase in PGE<sub>2</sub>  
155 release (Fig. 1B) which increased to 11.48- and 7.37-fold respectively in response to 10  
156 ng/ml IL-1 $\beta$  (Fig. S1A-B). Consistent with previous studies [5] this response was significantly  
157 reduced by mechanical loading in the form of CTS. IL-1 $\beta$  induced NO release was abolished  
158 by CTS such that there was no statistically significant effect at either 1 or 10 ng/ml (Fig. 1A,  
159 S1A). PGE<sub>2</sub> release was completely inhibited by CTS at 1 ng/ml IL-1 $\beta$  (Fig. 1B) but only  
160 partially suppressed at 10 ng/ml (Fig. S1B).

161 Simultaneous treatment with the TRPV4 antagonist GSK205 (10  $\mu$ M) abolished the anti-  
162 inflammatory effects of mechanical loading (Figure 1, S1). While GSK205 had no effect on  
163 NO or PGE<sub>2</sub> release in unloaded cells with or without IL-1 $\beta$ , in loaded cells the IL-1 $\beta$   
164 response was restored such that NO (Fig. 1A and S1A) and PGE<sub>2</sub> release (Fig. 1B, S1B)  
165 were significantly increased by IL-1 $\beta$ . Neither IL-1 $\beta$  nor GSK205 treatment in the presence  
166 or absence of CTS influenced TRPV4 protein levels (Fig. S10). These data indicate the anti-  
167 inflammatory effects of mechanical loading are mediated by TRPV4 activation.

168 **TRPV4 activation is required for the anti-inflammatory effects of hypo-osmotic loading**  
169 **in isolated chondrocytes and cartilage explants**

170 Isolated chondrocytes were treated with hyper-osmotic media (400 mOsm), hypo-osmotic  
171 (200 mOsm) or iso-osmotic media (315 mOsm) for 24 h (Figure 2AB, S2). Hyper-osmotic  
172 challenge had no significant effect on NO release, with or without IL-1 $\beta$  relative to the iso-  
173 osmotic control (Fig. S2, S3). By contrast, hypo-osmotic challenge significantly attenuated



174 the pro-inflammatory response to IL-1 $\beta$  (1 ng/ml), such that the increase in NO release at 24  
175 h was significantly reduced ( $p < 0.001$ , Fig. 2A S2A). Hypo-osmotic challenge had no  
176 apparent effect on cell viability compared to control conditions based on brightfield  
177 microscopy (Figure 2B). In the presence of GSK205, the anti-inflammatory effect of hypo-  
178 osmotic challenge on IL-1 $\beta$  induced NO release was completely inhibited by GSK205 such  
179 that the induction of NO release was not significantly different to control conditions (Fig. 2A).  
180 In the absence of IL-1 $\beta$ , GSK205 also had no effect on baseline NO or PGE<sub>2</sub> levels (Fig.  
181 S2).

182 In cartilage explants, hypo-osmotic challenge significantly reduced IL-1 $\beta$  induced NO release  
183 (Fig. 2C,  $p < 0.001$ ) such that there was no significant difference between IL-1 $\beta$  treated and  
184 untreated explants (Fig. 2C, S4A). In line with these findings hypo-osmotic challenge  
185 blocked the IL-1 $\beta$  mediated release of sGAG into the media, indicative of a reduction in  
186 extracellular matrix degradation (Fig. S4B). **Chondrocyte viability was maintained throughout**  
187 **the experiment as determined by live/dead staining (Fig. 2D)**. Consistent with isolated cells,  
188 hyper-osmotic challenge (400 mOsm, 12 d) had no effect on NO or sGAG release in the  
189 presence or absence of 1 ng/ml IL-1 $\beta$  (Fig. S4). GSK205 treatment restored IL-1 $\beta$ -induced  
190 NO release in hypo-osmotic media (Fig. 2C) thus blocking the anti-inflammatory effect of  
191 osmotic challenge. Interestingly, GSK205 further increased IL-1 $\beta$ -induced NO release in iso-  
192 osmotic, control media a response not seen in isolated cells (Fig. 2C). Together these data  
193 indicate the anti-inflammatory effects of hypo-osmotic loading are also mediated by TRPV4  
194 activation.

## 195 **TRPV4 activation is associated with altered primary cilia localisation and regulates** 196 **cilia length**

197 IL-1 $\beta$  induces primary cilia elongation in articular chondrocytes and mediates downstream  
198 catabolic NF- $\kappa$ B signalling through regulation of IFT [5, 23, 24]. We therefore examined the  
199 involvement of primary cilia in the anti-inflammatory mechanism of TRPV4 activation. TRPV4

200 cilia localisation was observed in isolated chondrocytes (Fig 3A). TRPV4 activation by  
201 mechanical loading, hypo-osmotic challenge or the TRPV4 agonist GSK101 (1 nM)  
202 increased TRPV4 cilia localisation while not significantly affecting protein expression, as  
203 shown by the increased mean intensity of ciliary TRPV4 (Fig. 3B, S10) and altered  
204 distribution profile of TRPV4 in proximal and distal regions of the axoneme (Fig. 3C) these  
205 data are suggestive of alterations in IFT.

206 In isolated chondrocytes, IL-1 $\beta$  (1 ng/ml) treatment for 24 h induced a significant increase in  
207 primary cilia length ( $p < 0.001$ ) from a median value of 2.21 to 2.84  $\mu\text{m}$ . This elongation was  
208 abolished by TRPV4 activation with GSK101 (Fig. 3D-E). IL-1 $\beta$  mediated cilia elongation  
209 was also blocked by mechanical loading (CTS, 0-10%, 0.33 Hz, Fig. 3G) and hypo-osmotic  
210 challenge (Fig 3H). Inhibition of TRPV4 with GSK205 restored IL-1 $\beta$  mediated cilia  
211 elongation in the presence of both mechanical loading ( $p < 0.001$ , Fig. 3G), and hypo-osmotic  
212 challenge ( $p < 0.001$ , Fig. 3H). GSK101, had no effect on cilia length in iso-osmotic conditions  
213 with or without IL-1 $\beta$  (Fig. 3E). GSK101 also had no effect on cilia prevalence for any of the  
214 treatment groups (Fig. S5A and D).

### 215 **TRPV4 activation inhibits inflammatory signalling in response to IL-1 $\beta$ through the** 216 **regulation of HDAC6 and ciliary tubulin**

217 We next examined whether direct pharmaceutical activation of TRPV4 would replicate the  
218 anti-inflammatory effect of mechanical and osmotic loading. IL-1 $\beta$  (1 ng/ml) induced the  
219 characteristic upregulation of NO and PGE<sub>2</sub> release in isolated chondrocytes which was  
220 abolished by GSK101 (Fig. 4A and B). Similarly IL-1 $\beta$  induced COX2 expression was  
221 abolished by GSK101 (Fig. 4C). No effects on cell viability based on bright field microscopy  
222 (Fig. S6A) and DNA content were observed although cells appeared to have a more rounded  
223 morphology particularly at high concentrations (Fig. S6B).

224 Previously, we identified a mechanistic role for HDAC6 activation and post-transcriptional  
225 tubulin modifications in the anti-inflammatory effect of mechanical loading [5]. Similarly,

226 GSK101 resulted in significant upregulation of HDAC6 activity (Fig. 4D) suggesting TRPV4-  
227 mediated calcium signalling activates HDAC6. Consistent with this finding we observed  
228 significant tubulin deacetylation accompanied by a reduction in the pool of non-polymerized,  
229 soluble tubulin (Fig. 4E-F). Furthermore, the HDAC6 specific inhibitor, tubacin (500 nM),  
230 restored IL-1 $\beta$  mediated stimulation of NO release in GSK101-treated cells (Fig. 4G). These  
231 data suggest that GSK101 mimics the effects of mechanical loading on IL-1 $\beta$  inflammatory  
232 signalling, HDAC6 activation and tubulin modification.

### 233 **TRPV4 activation abolishes IL-1 $\beta$ mediated cartilage degradation and loss of** 234 **mechanical properties**

235 We next determined whether pharmaceutical activation of TRPV4 could prevent cartilage  
236 degradation and loss of mechanical properties. Cartilage explants were treated with IL-1 $\beta$  for  
237 up to 12 d in the presence of 1 nM or 10 nM GSK101. Cartilage explant viability was  
238 maintained at these experimental doses (Fig. S7). In response to IL-1 $\beta$  treatment, significant  
239 NO release was observed (Fig. 5A,  $P < 0.001$ ) indicative of activation of inflammatory  
240 signalling. This response was accompanied by significant sGAG release indicative of  
241 cartilage degradation (Fig. 5B,  $P < 0.001$ ).

242 We measured the viscoelastic properties of cartilage tissue using uniaxial unconfined  
243 compression to determine whether GSK101 could prevent the loss of mechanical properties  
244 induced by IL-1 $\beta$ . Cartilage explants exhibited a non-linear stress-strain graph represented  
245 by a tangent modulus of 15-20MPa (Fig 5C). This was followed by characteristic viscoelastic  
246 stress relaxation at 20% strain (Fig 5D) to a relaxation modulus of 2-3 MPa at 300 s  
247 representing 80% relaxation and a relaxation half-life of approximately 50 s (Fig. 5E-H). IL-  
248 1 $\beta$  treatment resulted in dramatic loss of mechanical stiffness as shown by significant  
249 reductions in tangent modulus ( $p < 0.001$ , Fig. 5E) and relaxation modulus ( $p < 0.001$ , Fig. 5F),  
250 increased percentage relaxation ( $p < 0.001$ , Fig. 5G) and a reduction in half-life ( $p < 0.001$ , Fig.  
251 5H).

252 GSK10 significantly inhibited the cumulative release of NO from cartilage explants in  
253 response to IL-1 $\beta$  treatment ( $p < 0.001$ , Fig. 5A). Similarly the cumulative release of sGAG  
254 was significantly reduced ( $p < 0.001$ ) and loss of mechanical properties in response to IL-1 $\beta$   
255 abolished, such that there was no significant difference in any of the biomechanical  
256 parameters with and without IL-1 $\beta$ .

## 257 **Discussion**

258 This study demonstrates that TRPV4 plays an important mechanistic role in the anti-  
259 inflammatory effect of mechanical stimulation. TRPV4 inhibition restores IL-1 $\beta$  mediated pro-  
260 inflammatory signalling in the presence of both mechanical and osmotic loading. Conversely,  
261 TRPV4 activation by GSK101 blocked the release of pro-inflammatory mediators in the  
262 absence of load in isolated cells and prevented cartilage degradation and loss of mechanical  
263 properties in an explant model. TRPV4 is activated by mechanical stimulation in the form of  
264 cyclic tensile strain or osmotic challenge and functions upstream of HDAC6 to modulate  
265 tubulin acetylation and polymerization which regulates IFT thereby suppressing IFT-  
266 dependent IL-1 $\beta$  signalling.

267 TRPV4 is expressed in bone marrow stem cells, osteoblasts, osteoclasts and chondrocytes,  
268 and is required for skeletal development [10, 33]. TRPV4 belongs to the Transient Receptor  
269 Potential (TRP) superfamily which mediate cellular responses to a variety of environmental  
270 stimuli including heat [34], cell swelling [35], hypo-osmolality [18, 36] and mechanical  
271 loading [7, 9] and results in elevated levels of intracellular Ca<sup>2+</sup>. Thus, TRPV4 is required for  
272 mechanotransduction. It promotes chondrocyte matrix production in response to dynamic  
273 compression [7], mediates the fluid shear induced osteogenic response in stem cells [9] and  
274 shear stress induced vasodilatation in endothelial cells [8].

275 In other tissues, TRPV4 activation is mostly reported to be pro-inflammatory. In airway  
276 epithelial cells, TRPV4 activates NF- $\kappa$ B signalling promoting progression of lung fibrosis [37].  
277 Endogenous TRP channel agonists are detected in a lung injury model while TRPV4

278 inhibition suppresses acid-induced pulmonary inflammation [38]. TRPV4 antagonists have  
279 been used to treat sepsis in mice by reducing production of TNF- $\alpha$ , IL-1 and IL-6 [16].  
280 Moreover loss of TRPV4 function suppresses inflammatory fibrosis in mouse corneas [39].  
281 However, Xu et al. report that GSK101 prevents vascular inflammation and atherosclerosis,  
282 associated with inhibition of NO synthase and MAPK signalling [14]. TRPV4 is also well-  
283 established to mediate inflammatory hyperalgesia (see review [40]) and is regarded as a  
284 promising target for novel analgesics.

285 Consistent with our findings, pharmaceutical activation of TRPV4 has been shown to  
286 suppress NO release induced by lipopolysaccharide (LPS) in rat temporomandibular  
287 chondrocytes, whereas TRPV4 inhibition aggravates the inflammatory response to LPS  
288 [13]. Clark et al. report that TRPV4 deficiency induces inflammation and disrupts cartilage  
289 matrix homeostasis. As such, TRPV4<sup>-/-</sup> mice exhibit a severe sex-dependent osteoarthritis  
290 (male mice are more susceptible) while the isolated chondrocytes fail to increase Ca<sup>2+</sup> influx  
291 in response to hypo-osmotic challenge [11]. These mice exhibit a more severe obesity-  
292 induced osteoarthritis, compared to wild-type mice [12]. However other studies report  
293 osmotic challenge to be a pro-inflammatory signal. Hubert et al observed induction of IL-8 in  
294 response to both hyper and hypo-osmotic stress [41] while hypo-osmotic stimulation of  
295 TRPV4 promoted PGE<sub>2</sub> release in porcine chondrocytes [18] and the expression of IL-1 $\beta$   
296 and IL-6 in bovine intervertebral disc cells [36], suggesting a pro-inflammatory role of  
297 TRPV4. We did observe a mild, transient increase in NO release in this study at 3 h hypo-  
298 osmotic challenge however this had resolved and was not significantly different to the control  
299 at 24 h (Fig. S8). Interestingly we observed dose-dependent cytotoxicity of GSK101 with  
300 extended explant culture at concentrations above 10nM (Fig. S7). Low concentrations of  
301 GSK101 elicit multiple short peaks of Ca<sup>2+</sup> signalling, which is more physiological compared  
302 with the large, sustained peaks observed at higher concentrations which might explain this  
303 [42]. These observations suggest perhaps that only moderate, short-term modulation of  
304 TRPV4 will be chondroprotective.

305 Servin-Vences et al suggest TRPV4 mechanosensitivity is dependent upon the type of  
306 stimulus applied [6]. Our data supports this hypothesis, complete abolition of NO release in  
307 response to IL-1 $\beta$  was observed following application of cyclic tensile strain (Figure 1), while  
308 hypo-osmotic challenge merely attenuated the response (Figure 2) suggesting TRPV4  
309 activation may be regulated distinct mechanisms and to different extents. Vriens et al report  
310 that TRPV4 activation in response to cell swelling is dependent upon arachidonic acid  
311 release [43] whereas Servin-Vences et al suggest direct channel gating occurs in response  
312 to membrane deflection [6].

313 The mechanosensitive ion channel PIEZO1 reportedly induces TRPV4 channel opening [44].  
314 PIEZO1 is activated chondrocytes following injurious loading and is suggested to play a  
315 greater role in chondroprotection than TRPV4 [6, 45]. It is possible the more pronounced  
316 anti-inflammatory effects of cyclic tensile strain observed in this study are the result of further  
317 TRPV4 activation downstream of this channel, which could be explored in future studies.  
318 However, while activation of PIEZO1 reportedly influences ciliogenesis [46] studies in  
319 osteocytes indicate that it does not interact with TRPV4 in the cilium [47].

320 TRPV4 cilia localisation was observed with greater localisation evident at to the ciliary base  
321 (Fig. 3C). TRPV4 activation altered this distribution such that localisation to the base or tip of  
322 the axoneme was not significantly different indicative of altered protein trafficking/IFT (Fig.  
323 3C). TRPV4 activation is coupled with translocation of TRPV4 to plasma membrane [48], in  
324 this study we observed increased TRPV4 labelling in the ciliary membrane (Fig. 3AB).  
325 Chemical deletion of primary cilia with chloral hydrate fully abolishes Ca<sup>2+</sup> signalling in  
326 response to TRPV4 activation [18] thus increased ciliary TRPV4 may be important for  
327 signalling.

328 HDAC6 is enriched within primary cilia catalysing tubulin de-acetylation and polymerization  
329 to regulate cilia resorption [27-29]. In this study, mechanical, hypo-osmotic and  
330 pharmaceutical activation of TRPV4 blocked cilia elongation in response to IL-1 $\beta$ . IFT and

331 cilia elongation is required for IL-1 $\beta$  mediated inflammatory signalling and downstream NF-  
332  $\kappa$ B signalling [5, 23, 24], therefore we suggest the anti-inflammatory effects of TRPV4  
333 activation regulate IFT and associated signalling via HDAC6 dependent modulation of ciliary  
334 tubulin. Previous studies demonstrate that GSK101 activates Ca<sup>2+</sup> signalling in isolated  
335 chondrocytes [6, 17, 49], while GSK205 inhibits this response and blocks Ca<sup>2+</sup> signalling in  
336 response to mechanical or osmotic loading [18, 50, 51]. While Ca<sup>2+</sup> signalling was not  
337 assessed in the current study, we hypothesise that Ca<sup>2+</sup> levels may regulate HDAC activity  
338 through activation of upstream kinases such as Ca<sup>2+</sup>/Calmodulin dependent kinase (CaMK),  
339 protein kinase D (PKD) and Aurora A kinase-dependent (AURKA) [27-29, 52-55]. Studies  
340 suggest TRPV4 stimulation with GSK101 promotes ERK/MAPK signalling in lung epithelial  
341 cells and cancer cells [56] and PKC activity in endothelial cells [57] which phosphorylate  
342 HDAC6 resulting in increased deacetylation activity [58, 59]. Indeed, increased HDAC6  
343 activity was observed in response to GSK101 (Fig. 4D).

344 In conclusion, this study demonstrates a role for TRPV4 activation in the anti-inflammatory  
345 mechanism of loading. In addition to providing new mechanistic understanding of this  
346 pathway, this study identifies TRPV4 as a potential therapeutic target and demonstrates that  
347 pharmaceutical activation of this protein could regulate inflammation and other IFT-  
348 dependent pathways involved in cartilage disease.

### 349 **Acknowledgments**

350 We thank Dr Hannah Heywood for supplying the TRPV4 antagonist GSK205.

### 351 **Author contributions**

352 All authors aided in revising this manuscript for intellectual content and approved the final  
353 version to be published.

354 Study design: Su Fu, Clare L Thompson, Martin M Knight.

355 Data acquisition: Su Fu, Clare L Thompson, Sheetal Inamdar, Huan Meng

356 Data analysis and interpretation: Su Fu, Clare L Thompson, Sheetal Inamdar, Wen Wang,  
357 Himadri Gupta, Martin M Knight.

### 358 **Role of the funding source**

359 Su Fu and Huan Meng are funded by the China Scholarship Council for his PhD studies at  
360 Queen Mary University of London. Dr Clare Thompson is supported by a project grant from  
361 the UK Medical Research Council (No: MR/L002876/1, PI: Knight). Sheetal Inamdar is  
362 supported by a project grant from the Biotechnology and Biomedical Sciences Research  
363 Council (No: BB/R003610/1, PI: Gupta).

### 364 **Conflict of interest**

365 The authors have no competing interests.

### 366 **References**

367

368

- 369 1. Chen A, Gupte C, Akhtar K, Smith P, and Cobb J, The global economic cost of  
370 osteoarthritis: How the uk compares. *Arthritis*, 2012. 2012.
- 371 2. Knecht S, Vanwanseele B, and Stüssi E, A review on the mechanical quality of articular  
372 cartilage—implications for the diagnosis of osteoarthritis. *Clinical biomechanics*, 2006.  
373 21(10):999-1012.
- 374 3. Chowdhury TT, Bader DL, and Lee DA, Dynamic compression inhibits the synthesis of  
375 nitric oxide and pge(2) by il-1beta-stimulated chondrocytes cultured in agarose  
376 constructs. *Biochem Biophys Res Commun*, 2001. 285(5):1168-74.
- 377 4. Xu Z, Buckley MJ, Evans CH, and Agarwal S, Cyclic tensile strain acts as an antagonist of  
378 il-1 beta actions in chondrocytes. *J Immunol*, 2000. 165(1):453-60.
- 379 5. Fu S, Thompson CL, Ali A, Wang W, Chapple JP, Mitchison HM, et al., Mechanical  
380 loading inhibits cartilage inflammatory signalling via an hdac6 and ift-dependent



- 381 mechanism regulating primary cilia elongation. *Osteoarthritis Cartilage*, 2019.  
382 27(7):1064-1074.
- 383 6. Servin-Vences MR, Moroni M, Lewin GR, and Poole K, Direct measurement of trpv4 and  
384 piezo1 activity reveals multiple mechanotransduction pathways in chondrocytes.  
385 *Elife*, 2017. 6.
- 386 7. O'Connor CJ, Leddy HA, Benefield HC, Liedtke WB, and Guilak F, Trpv4-mediated  
387 mechanotransduction regulates the metabolic response of chondrocytes to dynamic  
388 loading. *Proceedings of the National Academy of Sciences*, 2014. 111(4):1316-1321.
- 389 8. Köhler R and Hoyer J, *Role of trpv4 in the mechanotransduction of shear stress in endothelial cells,*  
390 *in Trp ion channel function in sensory transduction and cellular signaling cascades*. 2006, CRC  
391 Press. p. 396-407.
- 392 9. Corrigan MA, Johnson GP, Stavenschi E, Riffault M, Labour MN, and Hoey DA, Trpv4-  
393 mediates oscillatory fluid shear mechanotransduction in mesenchymal stem cells in  
394 part via the primary cilium. *Sci Rep*, 2018. 8(1):3824.
- 395 10. Nilius B and Voets T, The puzzle of trpv4 channelopathies. *EMBO reports*, 2013.  
396 14(2):152-163.
- 397 11. Clark AL, Votta BJ, Kumar S, Liedtke W, and Guilak F, Chondroprotective role of the  
398 osmotically sensitive ion channel transient receptor potential vanilloid 4: Age- and  
399 sex-dependent progression of osteoarthritis in trpv4-deficient mice. *Arthritis Rheum*,  
400 2010. 62(10):2973-83.
- 401 12. O'Connor CJ, Griffin TM, Liedtke W, and Guilak F, Increased susceptibility of trpv4-  
402 deficient mice to obesity and obesity-induced osteoarthritis with very high-fat diet.  
403 *Annals of the Rheumatic Diseases*, 2013. 72(2):300-304.
- 404 13. Hu F, Zhu W, and Wang L, MicroRNA-203 up-regulates nitric oxide expression in  
405 temporomandibular joint chondrocytes via targeting trpv4. *Archives of oral biology*,  
406 2013. 58(2):192-199.
- 407 14. Xu S, Liu B, Yin M, Koroleva M, Mastrangelo M, Ture S, et al., A novel trpv4-specific  
408 agonist inhibits monocyte adhesion and atherosclerosis. *Oncotarget*, 2016.  
409 7(25):37622.
- 410 15. Pairet N, Mang S, Fois G, Keck M, Kühnbach M, Gindele J, et al., Trpv4 inhibition  
411 attenuates stretch-induced inflammatory cellular responses and lung barrier  
412 dysfunction during mechanical ventilation. *PLoS One*, 2018. 13(4):e0196055.
- 413 16. Dalsgaard T, Sonkusare SK, Teuscher C, Poynter ME, and Nelson MT, Pharmacological  
414 inhibitors of trpv4 channels reduce cytokine production, restore endothelial function  
415 and increase survival in septic mice. *Sci Rep*, 2016. 6:33841.
- 416 17. Kanju P, Chen Y, Lee W, Yeo M, Lee SH, Romac J, et al., Small molecule dual-inhibitors  
417 of trpv4 and trpa1 for attenuation of inflammation and pain. *Sci Rep*, 2016. 6:26894.
- 418 18. Phan MN, Leddy HA, Votta BJ, Kumar S, Levy DS, Lipshutz DB, et al., Functional  
419 characterization of trpv4 as an osmotically sensitive ion channel in porcine articular  
420 chondrocytes. *Arthritis Rheum*, 2009. 60(10):3028-37.

- 421 19. Qin H, Burnette DT, Bae YK, Forscher P, Barr MM, and Rosenbaum JL, Intraflagellar  
422 transport is required for the vectorial movement of trpv channels in the ciliary  
423 membrane. *Curr Biol*, 2005. 15(18):1695-9.
- 424 20. Wann AK, Zuo N, Haycraft CJ, Jensen CG, Poole CA, McGlashan SR, et al., Primary  
425 cilia mediate mechanotransduction through control of atp-induced ca<sup>2+</sup> signaling in  
426 compressed chondrocytes. *FASEB J*, 2012. 26(4):1663-71.
- 427 21. Kaushik AP, Martin JA, Zhang Q, Sheffield VC, and Morcuende JA, Cartilage  
428 abnormalities associated with defects of chondrocytic primary cilia in bardet-biedl  
429 syndrome mutant mice. *J Orthop Res*, 2009. 27(8):1093-9.
- 430 22. McGlashan SR, Haycraft CJ, Jensen CG, Yoder BK, and Poole CA, Articular cartilage  
431 and growth plate defects are associated with chondrocyte cytoskeletal abnormalities  
432 in tg737orpk mice lacking the primary cilia protein polaris. *Matrix Biol*, 2007.  
433 26(4):234-46.
- 434 23. Wann AK, Chapple JP, and Knight MM, The primary cilium influences interleukin-1beta-  
435 induced nfkappab signalling by regulating ikk activity. *Cell Signal*, 2014. 26(8):1735-  
436 42.
- 437 24. Wann AK and Knight MM, Primary cilia elongation in response to interleukin-1 mediates  
438 the inflammatory response. *Cell Mol Life Sci*, 2012. 69(17):2967-77.
- 439 25. Wann AK, Thompson CL, Chapple JP, and Knight MM, Interleukin-1beta sequesters  
440 hypoxia inducible factor 2alpha to the primary cilium. *Cilia*, 2013. 2(1):17.
- 441 26. Dinsmore C and Reiter JF, Endothelial primary cilia inhibit atherosclerosis. *EMBO Rep*,  
442 2016. 17(2):156-66.
- 443 27. Matsuyama A, Shimazu T, Sumida Y, Saito A, Yoshimatsu Y, Seigneurin- Berny D, et  
444 al., In vivo destabilization of dynamic microtubules by hdac6- mediated  
445 deacetylation. *The EMBO journal*, 2002. 21(24):6820-6831.
- 446 28. Thompson CL, Chapple JP, and Knight MM, Primary cilia disassembly down-regulates  
447 mechanosensitive hedgehog signalling: A feedback mechanism controlling adamts-5  
448 expression in chondrocytes. *Osteoarthritis Cartilage*, 2014. 22(3):490-8.
- 449 29. Ran J, Yang Y, Li D, Liu M, and Zhou J, Deacetylation of  $\alpha$ -tubulin and cortactin is  
450 required for hdac6 to trigger ciliary disassembly. *Sci Rep*, 2015. 5:12917.
- 451 30. Reed NA, Cai D, Blasius TL, Jih GT, Meyhofer E, Gaertig J, et al., Microtubule  
452 acetylation promotes kinesin-1 binding and transport. *Curr Biol*, 2006. 16(21):2166-  
453 72.
- 454 31. Dompierre JP, Godin JD, Charrin BC, Cordelieres FP, King SJ, Humbert S, et al.,  
455 Histone deacetylase 6 inhibition compensates for the transport deficit in huntington's  
456 disease by increasing tubulin acetylation. *J Neurosci*, 2007. 27(13):3571-83.
- 457 32. Thompson CL, Yasmin H, Varone A, Wiles A, Poole CA, and Knight MM, Lithium chloride  
458 prevents interleukin-1beta induced cartilage degradation and loss of mechanical  
459 properties. *J Orthop Res*, 2015. 33(10):1552-9.

- 460 33. Tanaka R, Muraki K, Ohya S, Yamamura H, Hatano N, Itoh Y, et al., Trpv4-like non-  
461 selective cation currents in cultured aortic myocytes. *Journal of pharmacological*  
462 *sciences*, 2008. 108(2):179-189.
- 463 34. Güler AD, Lee H, Iida T, Shimizu I, Tominaga M, and Caterina M, Heat-evoked activation  
464 of the ion channel, trpv4. *Journal of Neuroscience*, 2002. 22(15):6408-6414.
- 465 35. Becker D, Blase C, Bereiter-Hahn J, and Jendrach M, Trpv4 exhibits a functional role in  
466 cell-volume regulation. *Journal of Cell Science*, 2005. 118(11):2435-2440.
- 467 36. Walter B, Purmessur D, Moon A, Occhiogrosso J, Laudier D, Hecht A, et al., Reduced  
468 tissue osmolarity increases trpv4 expression and pro-inflammatory cytokines in  
469 intervertebral disc cells. *Eur Cell Mater*, 2016. 32:123.
- 470 37. Henry CO, Dalloneau E, Pérez-Berezo M-T, Plata C, Wu Y, Guillon A, et al., In vitro and  
471 in vivo evidence for an inflammatory role of the calcium channel trpv4 in lung  
472 epithelium: Potential involvement in cystic fibrosis. *American Journal of Physiology-*  
473 *Lung Cellular and Molecular Physiology*, 2016. 311(3):L664-L675.
- 474 38. Balakrishna S, Song W, Achanta S, Doran SF, Liu B, Kaelberer MM, et al., Trpv4  
475 inhibition counteracts edema and inflammation and improves pulmonary function and  
476 oxygen saturation in chemically induced acute lung injury. *American Journal of*  
477 *Physiology-Lung Cellular and Molecular Physiology*, 2014. 307(2):L158-L172.
- 478 39. Okada Y, Shirai K, Miyajima M, Reinach PS, Yamanaka O, Sumioka T, et al., Loss of  
479 trpv4 function suppresses inflammatory fibrosis induced by alkali-burning mouse  
480 corneas. *PLoS One*, 2016. 11(12):e0167200.
- 481 40. Grace MS, Bonvini SJ, Belvisi MG, and McIntyre P, Modulation of the trpv4 ion channel  
482 as a therapeutic target for disease. *Pharmacology & therapeutics*, 2017. 177:9-22.
- 483 41. Hubert A, Cauliez B, Chedeville A, Husson A, and Lavoigne A, Osmotic stress, a  
484 proinflammatory signal in caco-2 cells. *Biochimie*, 2004. 86(8):533-541.
- 485 42. Gilchrist CL, Leddy HA, Kaye L, Case ND, Rothenberg KE, Little D, et al., Trpv4-  
486 mediated calcium signaling in mesenchymal stem cells regulates aligned collagen  
487 matrix formation and vinculin tension. *Proceedings of the National Academy of*  
488 *Sciences*, 2019. 116(6):1992-1997.
- 489 43. Vriens J, Watanabe H, Janssens A, Droogmans G, Voets T, and Nilius B, Cell swelling,  
490 heat, and chemical agonists use distinct pathways for the activation of the cation  
491 channel trpv4. *Proc Natl Acad Sci U S A*, 2004. 101(1):396-401.
- 492 44. Swain SM, Romac JM, Shahid RA, Pandol SJ, Liedtke W, Vigna SR, et al., Trpv4  
493 channel opening mediates pressure-induced pancreatitis initiated by piezo1  
494 activation. *J Clin Invest*, 2020. 130(5):2527-2541.
- 495 45. Lee W, Leddy HA, Chen Y, Lee SH, Zelenski NA, McNulty AL, et al., Synergy between  
496 piezo1 and piezo2 channels confers high-strain mechanosensitivity to articular  
497 cartilage. *Proc Natl Acad Sci U S A*, 2014. 111(47):E5114-22.
- 498 46. Miyazaki A, Sugimoto A, Yoshizaki K, Kawarabayashi K, Iwata K, Kurogoushi R, et al.,  
499 Coordination of wnt signaling and ciliogenesis during odontogenesis by piezo type  
500 mechanosensitive ion channel component 1. *Sci Rep*, 2019. 9(1):14762.

- 501 47. Lee KL, Guevarra MD, Nguyen AM, Chua MC, Wang Y, and Jacobs CR, The primary  
502 cilium functions as a mechanical and calcium signaling nexus. *Cilia*, 2015. 4:7.
- 503 48. Cayouette S and Boulay G, Intracellular trafficking of trp channels. *Cell Calcium*, 2007.  
504 42(2):225-232.
- 505 49. Hurd L, Kirwin SM, Boggs M, Mackenzie WG, Bober MB, Funanage VL, et al., A mutation  
506 in trpv4 results in altered chondrocyte calcium signaling in severe metatropic  
507 dysplasia. *Am J Med Genet A*, 2015. 167A(10):2286-93.
- 508 50. Yu SM, Kim HA, and Kim SJ, 2-deoxy-d-glucose regulates dedifferentiation through beta-  
509 catenin pathway in rabbit articular chondrocytes. *Exp Mol Med*, 2010. 42(7):503-13.
- 510 51. O'Connor CJ, Leddy HA, Benefield HC, Liedtke WB, and Guilak F, Trpv4-mediated  
511 mechanotransduction regulates the metabolic response of chondrocytes to dynamic  
512 loading. *Proc Natl Acad Sci U S A*, 2014. 111(4):1316-21.
- 513 52. Youn H-D, Grozinger CM, and Liu JO, Calcium regulates transcriptional repression of  
514 myocyte enhancer factor 2 by histone deacetylase 4. *Journal of Biological Chemistry*,  
515 2000. 275(29):22563-22567.
- 516 53. McKinsey TA, Zhang CL, and Olson EN, Activation of the myocyte enhancer factor-2  
517 transcription factor by calcium/calmodulin-dependent protein kinase-stimulated  
518 binding of 14-3-3 to histone deacetylase 5. *Proceedings of the National Academy of  
519 Sciences*, 2000. 97(26):14400-14405.
- 520 54. Karppinen S, Hänninen SL, Rapila R, and Tavi P, Sarcoplasmic reticulum ca2+-induced  
521 ca2+ release regulates class iia hdac localization in mouse embryonic  
522 cardiomyocytes. *Physiological reports*, 2018. 6(2).
- 523 55. Pugacheva EN, Jablonski SA, Hartman TR, Henske EP, and Golemis EA, Hef1-  
524 dependent aurora a activation induces disassembly of the primary cilium. *Cell*, 2007.  
525 129(7):1351-63.
- 526 56. Nayak PS, Wang Y, Najrana T, Priolo LM, Rios M, Shaw SK, et al., Mechanotransduction  
527 via trpv4 regulates inflammation and differentiation in fetal mouse distal lung  
528 epithelial cells. *Respiratory research*, 2015. 16(1):60.
- 529 57. Baratchi S, Keov P, Darby WG, Lai A, Khoshmanesh K, Thurgood P, et al., The trpv4  
530 agonist gsk1016790a regulates the membrane expression of trpv4 channels.  
531 *Frontiers in pharmacology*, 2019. 10.
- 532 58. Du Y, Seibenhener ML, Yan J, Jiang J, and Wooten MC, Apkc phosphorylation of hdac6  
533 results in increased deacetylation activity. *PLoS One*, 2015. 10(4):e0123191.
- 534 59. Williams KA, Zhang M, Xiang S, Hu C, Wu J-Y, Zhang S, et al., Extracellular signal-  
535 regulated kinase (erk) phosphorylates histone deacetylase 6 (hdac6) at serine 1035  
536 to stimulate cell migration. *Journal of Biological Chemistry*, 2013. 288(46):33156-  
537 33170.

538

## **OSTEOARTHRITIS AND CARTILAGE**

### **AUTHORS' DISCLOSURE**

**Manuscript title** \_\_\_\_ Activation of TRPV4 by mechanical, osmotic or pharmaceutical stimulation is anti-inflammatory blocking IL-1 $\beta$  mediated articular cartilage matrix destruction. \_\_\_\_\_

Corresponding author Clare I Thompson

Manuscript number \_\_\_\_\_

#### **Authorship**

All authors should have made substantial contributions to all of the following: (1) the conception and design of the study, or acquisition of data, or analysis and interpretation of data, (2) drafting the article or revising it critically for important intellectual content, (3) final approval of the version to be submitted. By signing below each author also verifies that he (she) confirms that neither this manuscript, nor one with substantially similar content, has been submitted, accepted or published elsewhere (except as an abstract). Each manuscript must be accompanied by a declaration of contributions relating to sections (1), (2) and (3) above. This declaration should also name one or more authors who take responsibility for the integrity of the work as a whole, from inception to finished article. These declarations will be included in the published manuscript.

#### **Acknowledgement of other contributors**

All contributors who do not meet the criteria for authorship as defined above should be listed in an acknowledgements section. Examples of those who might be acknowledged include a person who provided purely technical help, writing assistance, or a department chair who provided only general support. Such contributors must give their consent to being named. Authors should disclose whether they had any writing assistance and identify the entity that paid for this assistance.

#### **Conflict of interest**

At the end of the text, under a subheading "Conflict of interest statement" all authors must disclose any financial and personal relationships with other people or organisations that could inappropriately influence (bias) their work. Examples of potential conflicts of interest include employment, consultancies, stock ownership, honoraria, paid expert testimony, patent applications/registrations, and research grants or other funding.

#### **Declaration of Funding**

All sources of funding should be declared as an acknowledgement at the end of the text.

#### **Role of the funding source**

Authors should declare the role of study sponsors, if any, in the study design, in the collection, analysis and interpretation of data; in the writing of the manuscript; and in the decision to submit the manuscript for publication. If the study sponsors had no such involvement, the authors should state this.

#### **Studies involving humans or animals**

Clinical trials or other experimentation on humans must be in accordance with the ethical standards of the responsible committee on human experimentation (institutional and national) *and* with the Helsinki Declaration of 1975, as revised in 2000. Randomized controlled trials should follow the Consolidated Standards of Reporting Trials (CONSORT) guidelines, and be registered in a public trials registry.

Studies involving experiments with animals were in accordance with institution guidelines

Please sign below to certify your manuscript complies with the above requirements and then upload this form at <http://ees.elsevier.com/oac/>

Author Signature	Date	Author Signature	Date
	06/01/2020		07/01/2020
	06/01/2020		13/01/2020
	21/01/2020		27/01/2020
	13/01/2020		17/06/2020



Click here to access/download

**ICMJE COI form**

OAC ICMJE coi\_disclosure\_thompson.pdf

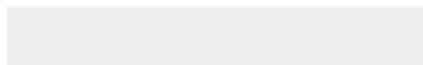




Click here to access/download

**ICMJE COI form**

OAC ICMJE coi\_disclosure\_knight.pdf







Click here to access/download

**ICMJE COI form**

OAC ICMJE coi\_disclosure \_Gupta.pdf

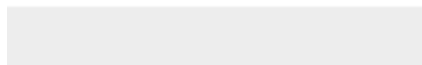




[Click here to access/download](#)

**ICMJE COI form**

**OAC ICMJE coi\_disclosure \_Wang.pdf**

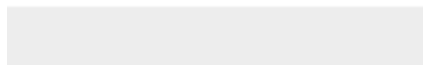




[Click here to access/download](#)

**ICMJE COI form**

[OAC ICMJE coi\\_disclosure\\_Fu.pdf](#)





Click here to access/download

**ICMJE COI form**

OAC ICMJE coi\_disclosure\_Inamdar.pdf

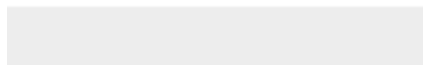




Click here to access/download

**ICMJE COI form**

OAC ICMJE coi\_disclosure \_Bijoy Das.pdf





[Click here to access/download](#)

**ICMJE COI form**

[OAC ICMJE coi\\_disclosure\\_Meng.pdf](#)

